symmetry

MDPI

Article

Methodologies to Determine Geometrical Similarity Patterns as Experimental Models for Shapes in Architectural Heritage

Juan Moyano [1,*], María Fernández-Alconchel [1], Juan E. Nieto-Julián [1] and Manuel J. Carretero-Ayuso [2]

[1] Department of Graphical Expression and Building Engineering, University of Seville, Ave. Reina Mercedes, 4A, 41012 Seville, Spain
[2] Department of Arquitecture, Arquitecture School, University of Alcalá, C. Sta. Úrsula, 8, 28801 Alcalá de Henares, Spain
* Correspondence: jmoyano@us.es

Abstract: Today, plans to protect historic buildings focus on managing architectural heritage sustainably. Technical teams, such as architects and restorers, use massive data acquisition techniques, so an identification mechanism is required to select geometrical similarity patters to support hypothesis that guarantee historical data. Moreover, computational methods are required to understand the role of organic shapes in historic buildings. This paper first describes an extensive review of the literature and then the algorithms and methods to compare and to detect similar geometrical elements and complex patterns in architecture and archaeology. For this purpose, two key aspects are considered: the metric standpoint and historical-graphical features of the 3D models, i.e., composition, techniques, styles, and historical-graphical documentary sources. Research implies testing several methodological lines to know the similarity degree of complex organic shapes in architectural details through statistical analysis, software to assess point clouds, and complex curve analysis. The results have shown that the three procedures can be compared and that the bases of the pillars of both the Cathedral of Seville and the churches in Carmona, Jerez, and Morón are very similar; however, the base of the pillar of the church in Carmona presents scalability variations.

Keywords: 3D range scanning; Terrestrial Laser Scanning; Structure-from-Motion; 3D data comparison; Cathedral of Seville

Citation: Moyano, J.; Fernández-Alconchel, M.; Nieto-Julián, J.E.; Carretero-Ayuso, M.J. Methodologies to Determine Geometrical Similarity Patterns as Experimental Models for Shapes in Architectural Heritage. *Symmetry* **2022**, *14*, 1893. https://doi.org/10.3390/sym14091893

Academic Editor: Jan Awrejcewicz

Received: 11 August 2022
Accepted: 6 September 2022
Published: 9 September 2022

1. Introduction

One of the key goals to preserve cultural assets is implementing preservation natural landscapes and all the artistic and historical elements created by mankind over time in research. Cultural heritage (CH) is a substantial and dynamic deposit of knowledge, considered as a unique and irreplaceable source of aesthetic, historical, and cultural values [1], so it should be documented to maintain the object and its knowledge. Consequently, works included in an architectural context are considered a worldwide category, as well as working areas of universal value. The architectural heritage composed of buildings, civil structures, and their objects, among others, is part of that unique value due to their nature. In this context, new digital tools foster the collaborative work among work teams and allow both the information related to the record of cultural assets and the accuracy of geometrical shapes to be managed. The digital record by using techniques to acquire accurate data is an interesting field for engineers and architects that work within the heritage area [2], so today, there are many works [3–9] focused on the applicability of photogrammetry techniques, such as Structure-from-Motion (SfM) and new Structure from Motion/Multi-View-Stereo (SfM/MVS) implementation algorithms, making such modeling easier from photo or video surveys [10–12] and techniques of Light Detection And Ranging (LiDAR) as Terrestrial Laser Scanning (TLS). Structure-from-Motion reconstruction methods can be used in order to retrieve complete surfaces with high precision, dense image matching methods. However, a key challenge is the selection of images, since the image network geometry directly

impacts the accuracy, as well as the completeness of the point cloud. Thus, the image stations and the image scale have to be selected to carefully meet the accuracy requirements. Furthermore, most dense image matching solutions are based on multi-view stereo algorithms, where the matching is performed between selected pairs of images [13]. In addition, the progress in architectural heritage within the field of 3D digital reconstruction has been related to surface analysis methods [14–16] for architectural shapes. Müller et al. [17] suggested fifteen years ago that manual methods are the best way to process details of shapes such as bricks or capitals, but today, the complex geometry of historic buildings is studied through the automatic procedure of Building Information Modeling (BIM) digital platforms. Thus, combining Massive Data Capture Systems (MDCSs) and the record in Heritage Building Information Modeling (HBIM) platforms constitutes an appropriate procedure to record elements such as columns, capitals, or arches, among other elements of the Gothic architecture. HBIM is the new paradigm in the scientific community because semantic components can be included. These components are represented as digital objects with relations, attributes, and properties [18], and geometry plays an important role in cultural heritage as most buildings have structural damages and deformations.

Thus, accuracy in geometry implies a greater analysis, with many sides and applications. However, the various scanning methods give advantages to study copies or digital twins with both a 3D detail and an incredible accuracy. The information provided by 3D digital models could replace the current iconographic material in cultural heritage [19], thus leading to both geometrical accuracy and important research studies that could be significant to determine authorships and to relate architectural shapes in the context of CH. To acquire that knowledge, this paper suggests describing algorithms and methods to compare and establish a geometric similarity pattern. The work will be based on comparing profiles of the geometric shapes by using algorithms through the CloudCompare software [20], calculating probability indexes through linear regression statistics and refuting the results with historical hypotheses of authorships and artistic styles. As we know CloudCompare is an open-source software with certain point cloud classification, segmentation, and evaluation algorithms derived from LiDAR or close-range photogrammetry, which allow (i) rasters based on LiDAR attributes, (ii) 3D vectors, (iii) changes of point cloud format, (iv) three-dimensional models, (v) point cloud self-classification, and (vi) data georeferencing. Therefore, a powerful tool widely used by the scientific community is the most used ICP algorithm. The nearest point algorithm based on the search for pairs of points in two adjacent scans. Reference [21] is open source and has been used by numerous researchers in evaluation studies, including for Scan-to-BIM [22,23] or structural behavior analysis [24,25].

The applications in archaeology and CH protection defined by Li and Zha [26] are the creation of digital files, 3D line drawing, and 3D virtual restoration. On the one hand, general files constitute new documents preserved for future intervention projects. On the other hand, 3D line drawing allows geometrical or organic shapes to be decoded to determine complex drawings in sculptures, and 3D virtual restoration allows orthophotos and Digital Elevation Model (DEM) or Digital Terrain Model (DTM) to be obtained from the 3D model, which includes detailed and accurate information in the digital plan of the archaeological excavation [27,28]. Moreover, there are studies that implemented 3D to analyze archaeological objects, such as [27,29–31], which determined the similarity of geometrical shapes, or [32], which developed software to determine the axis of rotation of the pottery made with wheels from several historical periods. To assess the characterization of the pottery, [33] determined a "*qp*" ("Quantum Platform" open-code software [34]) of the tool capable of producing in a semiautomatic way a 3D pot collection through the morphological characteristics of the old Greek pottery. Afterwards, a descriptor was designed. It was based on both nearly complete 3D vessel replicas [35] and Zernike Moments 2D (ZMDM) and Character-Based Depth Map Enconding (CBDM) depthmap descriptors [30]. Copies are compared not just by using specialized software, but recording methods between data acquisition techniques and old drawings to verify dimensionally

architectural shapes [36] or to compare old Roman coins by analyzing the deviation in the morphology of the surface of the coin [37].

From very valuable tools for capturing images, the development in geometric morphometry (GM) appears, a tool through which it is possible to abstract the shape of organisms through the use of "marks or points" and where the size, position, and orientation are adjusted to obtain the information of the "shape of its outline" in a mathematical context. The applicability was initiated by biologists to characterize the size and shape of living things. The essence focuses on reducing the shape of the entire object to a set of individual points called reference points [38,39] that will mark the biological structure of the shape. Like any process that occurs in the lines of research, the methodology of the medical-forensic area of skull characterization studies passes to the archaeological study through the analysis of the stone. The way to characterize the shape of the lithic stone through the use of reference points can be seen in the work of [40].

The historiography suggests analyzing similar architectural shapes based on the computational study by Pintus et al. [41]. The problems in observing shapes and interpreting objects are among the goals of this study, focused on the geometric classification criteria and the cardinality of the relations between the areas of the objects. In another line, several research studies are focused on the analysis of symmetries in architecture. An example is the study of automated Architectural Symmetry Detection (ASD), suggesting an information model of the cities to model digital twin objects from a Light Detection And Ranging (LiDAR) point cloud [42].

Both the texture of architectural design arrangements and the relationship between their surface have been widely studied by means of fractal pattern techniques [43–45]. Nevertheless, it is a metric-characterized geometrical analysis that does not comply with the scope of this research. In this regard, the authorship of stonemasons and master builders in the Gothic architecture is not generally allocated due to the lack of sources, such as factory books. The use of new technologies based on the analysis of architectural shapes could be a mechanism to make authorship hypotheses that identify pieces carved by the same stonemason or designed by the same master builder.

This research started from a work [46] which studied the similarity of patterns through the linear regression statistics. Afterwards, the algorithms were analyzed by using the software CloudCompare by algoritm ICP and mathematical geometry models, and the analysis has also been extended to two churches that contain historical aspects of the Gothic architecture of the lower Guadalquivir River. The next step is to provide new methodologies related to the formal analysis based on data acquisition methods, as well as to compare new scenarios of case studies that are an original document.

Thus, characterizing architectural shapes based on morphological similarities is an important experimental field to classify not just archaeological pieces, but also architectural pieces used both to identify replicas through their relations with previous periods and to determine historical hypotheses. Based on the MDCSs, procedures are established to compare the shapes of the bases of the pillars of four churches (Figure 1a) and their location (Figure 1b). This procedure is based on similarity statistics, the determination of homologous points, and the agreement of characteristic sections and characteristic points.

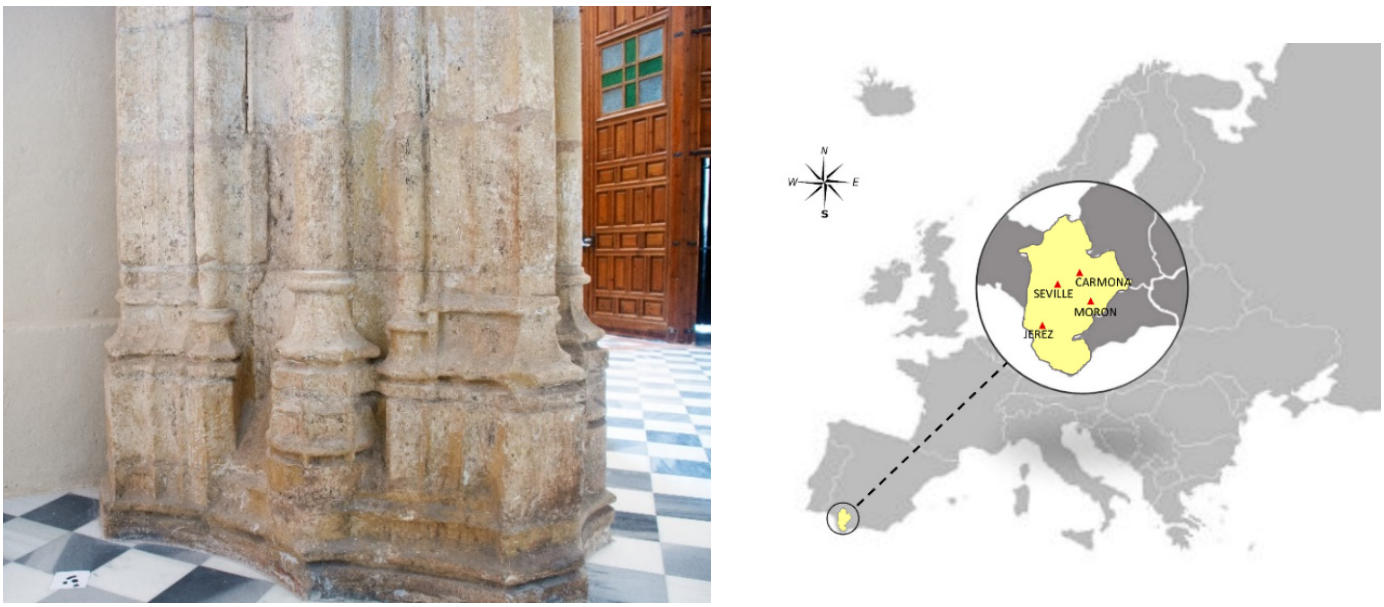

(**a**) (**b**)

Figure 1. (**a**) Photograph of the pillar of the church in Morón de la Frontera. (**b**) Location of Seville cathedral and other gothic churches.

Like 400 years ago, stonemasons or master builders involved today in the restoration of cathedrals and churches verify the cut of the stone by using tools, such as rigid and articulated squares, wooden and cartoon templates, and graduated and curved rules. All these tools are used by stonemasons. These objects, which are museum pieces, such as the Anglican cathedral in Liverpool, St James Mt Cathedral, with many pieces used in its construction in the 20th century, are the easiest way of transmitting the Euclidean geometry and are the responsible for creating art based on geometric shapes in which lines and arches forming its geometry are inseparable of the structural function [47]. Many of the studies by authors such as Alonso de Valdelvira [48] and Hernán Ruiz "el Joven" [49] showed the importance of the architectural graphic expression in the treaties of Gothic architecture. Many of these studies interpret the geometric design of vaults, stairs, arches, and pillars built with stone using a hammer. The most recent historiography includes researchers focused on Gothic designs [50], which maintained the hypothesis on the geometries of ribbed vaults through the Euclidean geometry. The studies by the Sevillian researcher specialized in tracings in heritage buildings are also interesting [51,52]. These studies showed that the material control of the productive process of the design of the stone is based on the line [53] as its traditional execution in the Gothic period. The geometry of shapes in a stonework is verified through proportions, scale, and the design of the line and the curve. Today, the vision of the digital twin refers to the physical and functional description of a component which includes all the information of its useful life [54]. In this regard, the geometric control components could also be used as a digital twin to provide information on the material with purposes of structural engineering. Thus, the bases that are part of the beginning of the pillars of the churches and cathedral already mentioned were chosen. This decorative element in Figure 2 obtained from the base of the pillar (Figure 3) represents one of the geometries in which stonemasons should sculpt at the beginning of the historical construction. In these case studies, researchers have worked with very similar structures, although scales slightly vary. For this reason, this study is first focused on the characteristic points to determine a geometric similarity pattern.

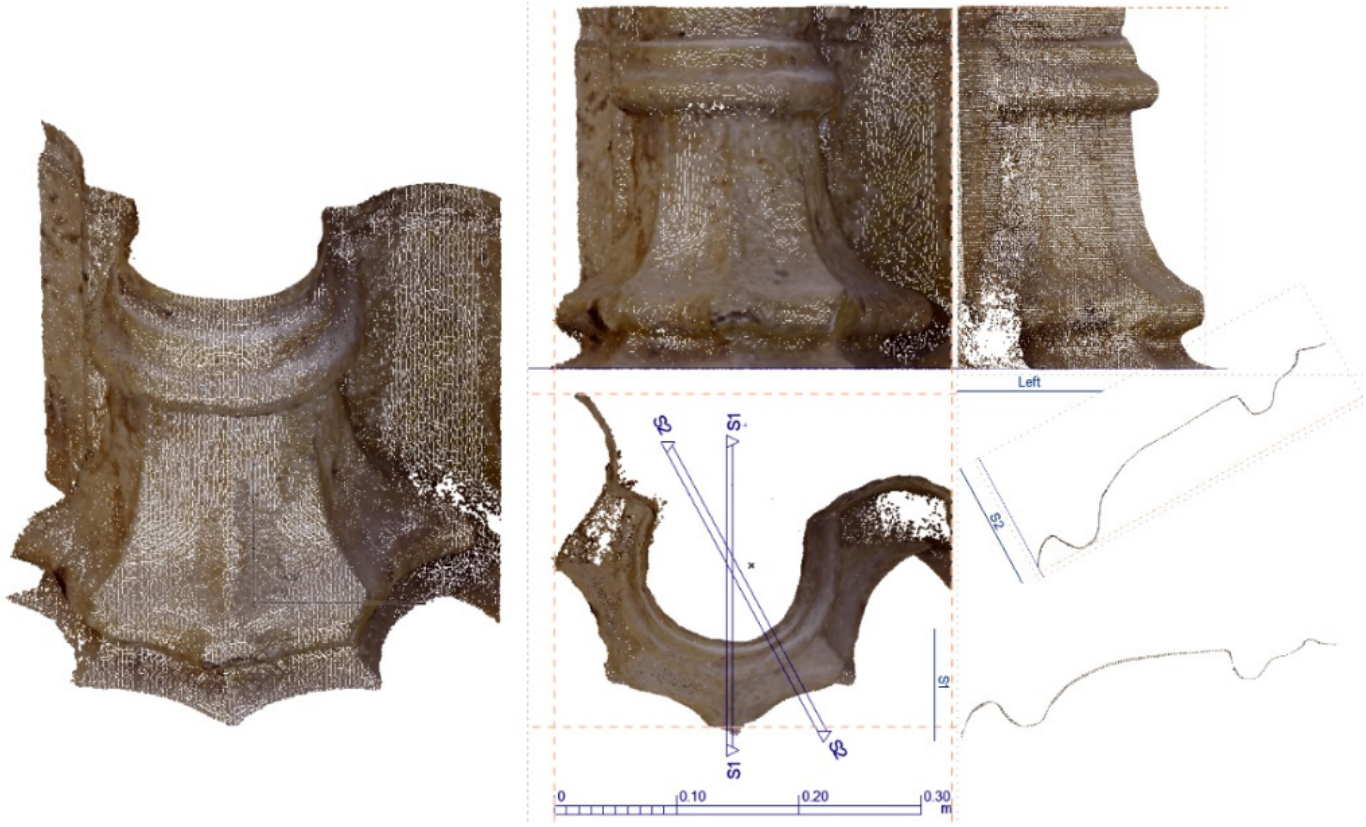

Figure 2. Projections of the base of the church in Carmona.

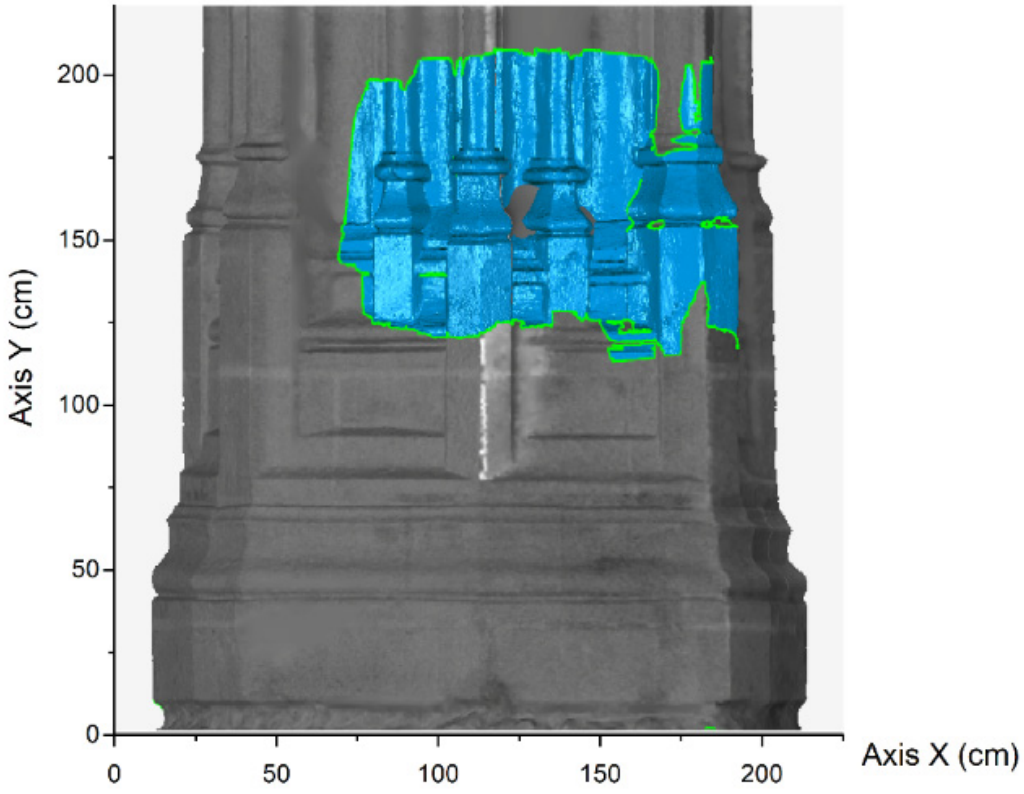

Figure 3. Sector scanned and coupled to the TLS of the church in Jerez.

2. Case Studies

The similarity of the Gothic shapes of the Cathedral of Seville and other bordering churches could be seen in the decorative program of traceries, capitals, and frames used in the construction of posterior temples. The clearest examples are the Santiago Church in Jerez de la Frontera, whose master builder, Alonso Rodríguez, author of the design, worked at the end of the 15th century and at the beginning of the 16th century to erect the structure of the church [55]. In the historiography of the Cathedral of Seville, both Falcón [56] and Sancho de Sopranis considered the Cathedral of Seville as the inspiring building of the church in Jerez. There are very clear similarities in the apse and in the structure of the church. The San Miguel Arcángel Church in Morón de la Frontera was built in two periods between 1506 and 1730. It is classified within the select group of historic buildings of the cathedral Gothic [57], in which the masters projected and disseminated the architectural details made in the Cathedral of Seville in the 15th century. The Nuestra Señora de la Asunción Church, in Carmona, was also built under the influence of the Cathedral of Seville at the end of the 15th century. It has three naves, side chapels and a slightly rectangular plan. It was started by the front, like the Cathedral of Seville, maintaining the old *sahn* or ablution yard of the mosque. The church in Carmona is considered one of the main temples that represents the Late Gothic based on the Cathedral of Seville [58]. In recent investigations [59], other types have been found that are very similar to these forms of construction of the Gothic style of their bases, for example, the Church of the Divine Savior of Vejer de la Frontera, but here the base is more stylized. In addition to the ecclesiastical ensembles of the Late Gothic Mediterranean environment, there is the Cathedral of Palencia where Ysambart, master stonemason in 1433 in Seville, worked together with Pedro Jalopa in the splendid funerary chapel of the Saldaña [60]. The authors compare profiles and try to find similarities between the shapes. The choice of these profiles is made because of the similarity of the forms exposed by the historiography of the Cathedral of Seville, selecting four representative samples by means of their cross section.

3. Data Acquisition

As for the scope of geomatics and topography, control points determine an essential space in the measurements of the architectural and archaeological objects. Thus, the control points are widely used for the formal control of the architecture. In "classical" SfM/photogrammetric pipeline, control points are used for image orientation in the assumed reference system. For indented assessment, check points are utilized. In the close-range photogrammetry, the complementary value of the Ground Sample Distance (GSD) in the use of Digital Elevation Models (DEM) has a determinant space [61]. Moreover, [62] revealed the difficulty in arranging control points for georeferencing; [63] reviewed the advantages of direct georeferencing in point cloud achievement for complex elements and geometries and Devrim Akca et al. [64] addressed the verification of the data used by means of quality control in 3D modeling. In this regard, to locate the work in the set, points existing in other records were used as reference. These points were used to georeferenced the scan to the city plans by means of a total station. As the column bases scanned contain surfaces with sufficient geometrical magnitude, targets to link the different scans were not set. TLS was the technique used for this purpose: a Leica ScanStation C10 laser scanner, with 5 mm resolution and 2 mm accuracy (in accordance with Leica Geosystems specifications). The applicability of the terrestrial laser scanner and the structured light scanner is used for presentation purposes context since the true analysis is carried out through photogrammetry.

Regarding photogrammetry, knowing some aspects about the way of working is crucial. Thus, the superposition among adjacent photographs should be guaranteed [65] and the distance from the object should be established, so the GSD should be nominal [66]. The recommendations given in the data capture section are appropriate in the studies focused on architectural heritage in a classification of Class A, according to Campos [67]. Images were processes through Darktable [68], an open-code software to develop pho-

tographs. Afterwards, Agisoft Metashape [69] was used for 3D image processing through control points taken by the total station LEICA Flexline TS02, with a precision of 2 mm [70]. The full description of the SfM method is that used in previous studies [71], which are based on the detailed description given by Jaud [72]. Figure 4 shows a 3D digital model of the pillar of the church in Morón made through photogrammetry. The surveys of the low pillar of each church were conducted with the digital reflex camera NIKON D80, with a 12 MP sensor, with the following size: 23.6–15.6 mm, lens Nikon DX AF-S NIKKOR 18–135 mm f/3.5–5.6 G E, and a tripod. The focal distance was 18 mm, stabilizer of optical image and (fixed) exposition 1/400 sf 3.5. The size of the CCD sensor was 23.6 mm × 15.8 mm, distributed in 3872 × 2592 pixels for a maximum resolution in NEF RAW format. The ISO value was set to 200. With respect processing configuration the steps are developed in: (i) Match photos Chunk. Align cameras with parameter "Accuracy High (full resolution image files)". (ii) Build Dense cloud with parameter "Quality High". (iii) Build mesh with parameter "Source date Depth maps". (iv) Build DEM with parameter projection Type Geographic". The GCPs were placed both in the part of the horizontal plane and distributed among the elements of the pillar in such a way that the total station could capture all of them in a single position. The XYZ coordinates set were 100, 100, and 10 m. The coordinates of the elements on each space were later recorded to achieve a uniform set of points. In the processing SfM, an accuracy of 0.001 m was recorded.

Figure 4. Three-dimensional digital model from the photogrammetry of the pillar of the church in Morón de la Frontera, Spain.

The combination of the techniques based on images and ranges have complementary advantages [73] as the attributes provided by photogrammetry are complementary to those provided by the TLS as accurate data acquisition. For this reason, and to know the general context of the columns, the column was recorded by using TLS, and the level of detail of the base was scanned with the Artec MHT 3D scanner, as Figure 5 shows. Through a field of view of 214 mm × 148 mm (high × width) and distant 536 mm × 371 mm, the scanner provides a resolution of 1 mm to create three-dimensional meshes that could be textured. This optical use has been used in many records both for medicine [74] and for the scanning

of small objects, such as sculptures [75]. In addition, methods such as the optical flow [76] or the digital image correlation (DIC) [77] could be used to know the deformations of the changes in the case of the photogrammetry point cloud or a digital model.

Figure 5. Meshed 3D model of the pillar of the Santiago Church in Jerez de la Frontera by using Artec Studio 10 Professional.

Although many tools of Massive Data Capture Systems (MDCSs) were used, the models used for the assessment were photogrammetry, which guarantees a more homogeneous resolution of characteristic points of the point cloud, comparing the cloud in just one range and limiting the comparison to the simple share, without including variables, such as uncertainty, due to instrumental errors. Both TLS and Optical Flight Model (OFM) have made auxiliary 3D reconstruction, but in this case, they have not been used to analyze the dataset. Photogrammetry provides characteristic attributes of the point cloud, such as x, y, z coordinates, RGB colors, and also the three normal directions such as the remaining techniques. Thus, a dynamic point cloud could be treated as a sequence of various static point clouds, but all in their own context [78].

The resulting meshes were finally aligned and located in their accurate location on the global point clouds of each base. Figure 5 shows the result of this process. The meshing was carried out with Agisoft Metashape, a photogrammetry software in the post-processing of the record. To know the point cloud used in the methodology, Figure 6 is shown in two different models, appreciating the scale of both objects.

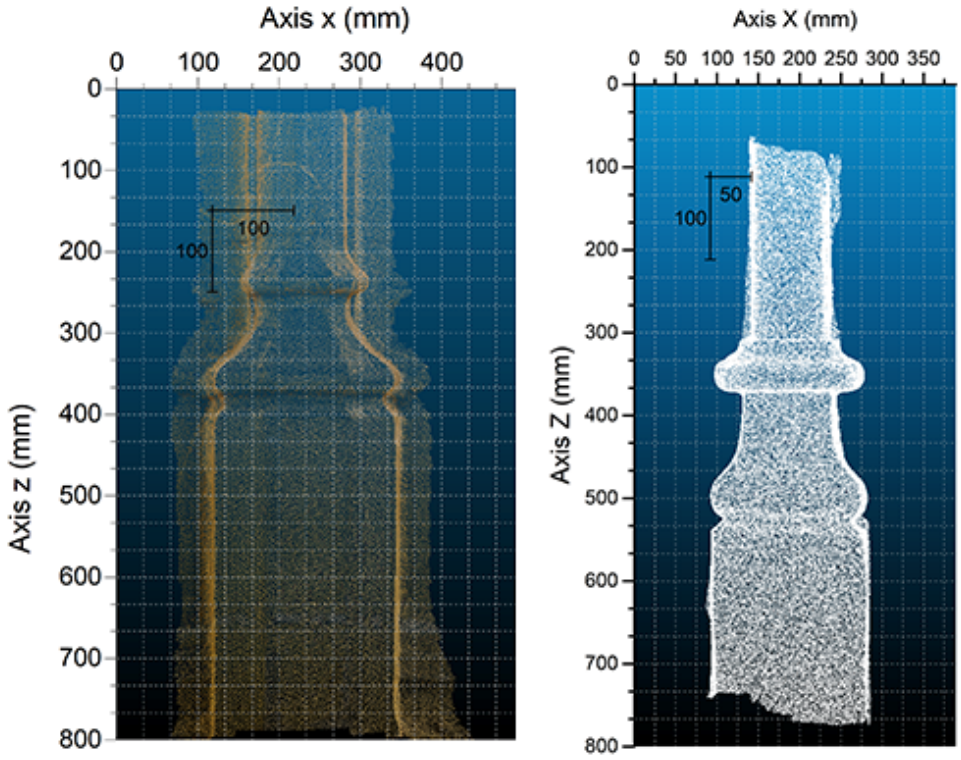

(**a**) (**b**)

Figure 6. (**a**) Image of the set of points obtained from SfM of the church in Carmona; (**b**) image of the set of points obtained from TLS of the church in Jerez de la Frontera.

4. Methodological Analysis and Results

The methodology of this work is based on the original idea of both establishing characteristic points in the geometry of the objects and comparing these points. The shapes analyzed were certain sections of the bases of the pillars of the Cathedral of Seville, the Santiago Church, the church in Morón, and the church in Carmona. There are curves in these sections that determine characteristic points that are accurately used by stonemasons to work the stone. The original points were analyzed and compared with the coincident points in each case. There are two key aspects in the methodology: i) from the point of view of the methodological and historical characteristics, and ii) the coincidence of the metric scalability.

Although there are diverse experiences, ad-hoc algorithm proposals and point cloud comparison techniques [79], the first step in the analysis was the CloudCompare (C2C) software package [20], which is useful to manage and compare point clouds [21]. The comparison between the organic shapes was maintained in an adjustment of the curves in 2D (AutoCAD) software and exported to C2C, with axes of coordinates and slopes previously established by the authors. Thus, the points of the curves were not aligned because their importance was referenced to an axis of coordinates. The geometric deviation was calculated through the distances from cloud to cloud in C2C, which calculated the distance from each point, in this case from the data subsets of shape P_c to shape P_m, both obtained through the SfM cloud by the Agisoft Metashape software [80]. The results of the surveys are shown in the histogram in the axis of abscissas, and the number of points is shown in the ordinate axis. The study sequence was based on the comparison of the model of the Cathedral of Seville with the other geometries. The first one is between Seville and Morón, which determined the deviations as Figure 7 shows.

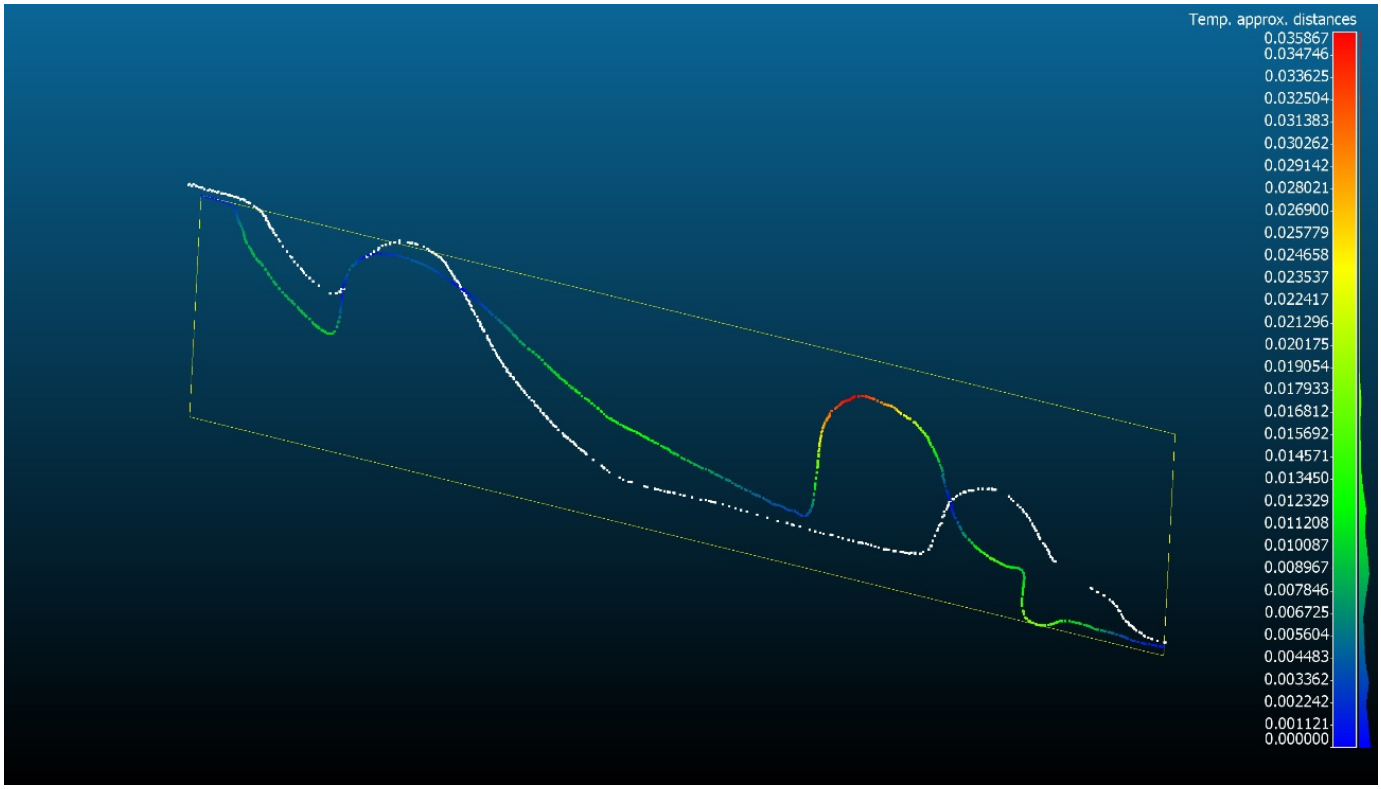

Figure 7. Image of the deviations between the profile Seville-Morón. Data from the comparison C2C absolute distance between profile. Unit: meters (X-axis). Visualization mode. Heat maps of distance distributions.

The average distances between the two data subsets of the two-point clouds generated through profiles of a global point cloud (TLS_i) Y were calculated (Figure 8). The parameters studied were the root mean square (RMS), the minimum and maximum distances between the point clouds, the average distance, the standard deviation, and the standard error estimated in meters. According to [81], the deviation between similar objects presents two main characteristics: on the one hand, the high presence in the zero value in comparison with the intervals of distance and, on the other hand, the standard deviation, which could be calculated according to the formulae provided by [82], used in other studies [71,83] and defined in 1984 by [84] (Equation (1)) of the points along those intervals.

$$\sigma = \sqrt{\frac{1}{n-1}\sum_{i=1}^{n}(x_i - \overline{x})^2} \quad (1)$$

where n is the sample size, x_i are the points in the intervals, and $\overline{x}$ is the average sample value.

The accuracy of the tools used and the optimization of characteristic points by means of the mean squared error (De Reu et al., 2013) were empirically considered. A sample of the points and the sections of the elements in the Cathedral of Seville are displayed in Figures 8 and 9.

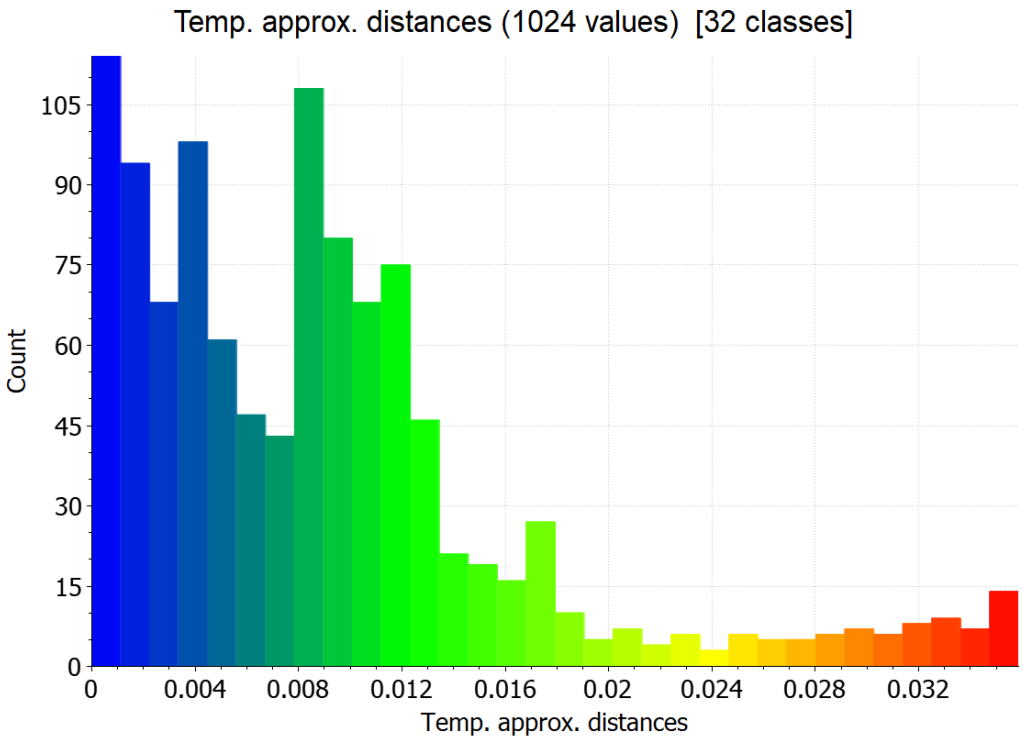

Figure 8. Histogram plot. Deviations between the profile Seville-Morón. Units: meters (X-axis) and number of points (Y-axis).

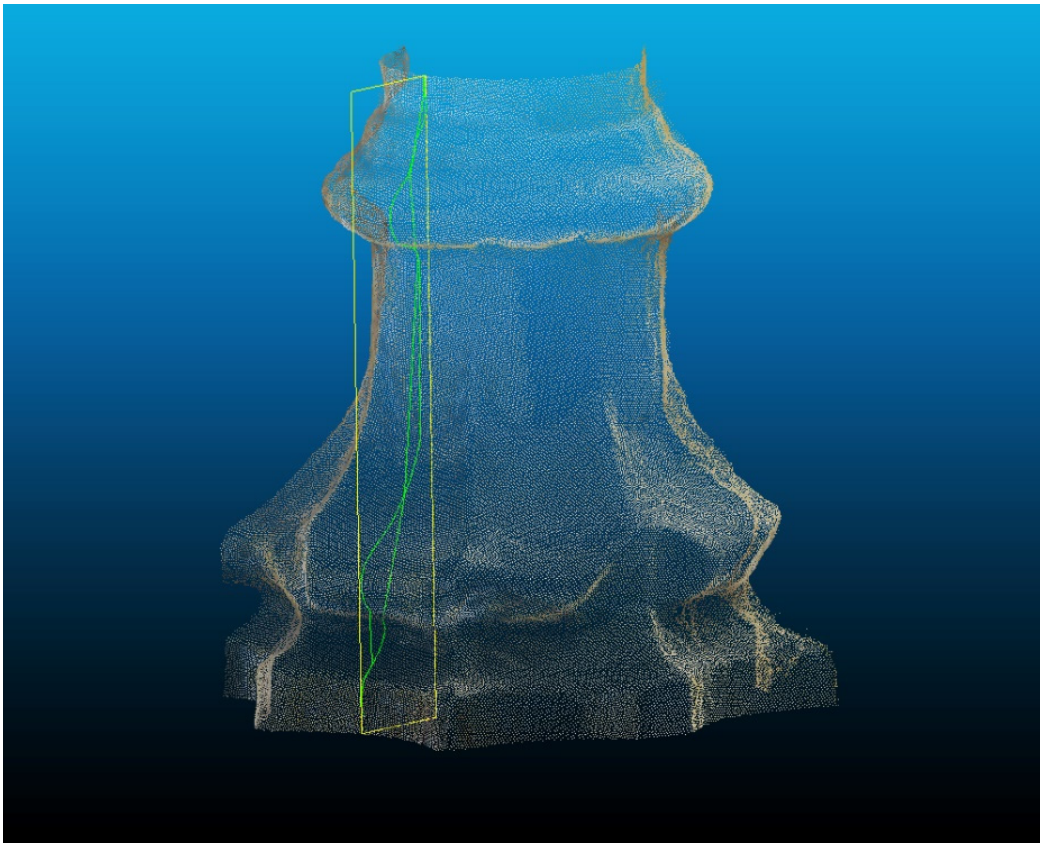

Figure 9. Vertical section generated through Cloud Compare and the applicability of points in the space.

The points of the profile P_c (capture of the subset of the points of the base of the Cathedral of Seville) were compared with the profiles of P_m (capture of the subset of the points of the base of the church in Morón de la Frontera) using the distance tool from cloud to cloud in CloudCompare. This algorithm calculates the Hausdorff distance between the referential point cloud and the points closer to the other cloud [85], thus calculating the distance [20].

$$d\ (p_x,\ S_0) = min\|p_x - p_0\| \tag{2}$$

where p_x is a point of S_x and p_0 is the closest point of p_x in S_0. Apart from the distance, the output of the algorithm provides the displacement vector between p_0 and p_x. This vector was then used to obtain the horizontal and vertical changes between t_0 and t_x. Table 1 includes the results of the comparison of the various profiles, as well as the average deviations, the errors, and the maximum and minimum values among the various profiles p_x.

Table 1. Results obtained from the comparison of the various profiles.

Experimental Surveys	Standart Deviation (σ) (m)	RMS (m)	Min. Distance (m)	Max. Distance (m)	Average Distance (m)	Estimated Standard Error (m)
C. Sevilla-C. Carmona	0.0110	0.0120	0	0.0440	0.0120	0.0010
C. Sevilla-C. Morón	0.0080	0.0110	0	0.0360	0.0080	0.0010
C. Sevilla-C. Jerez	0.0060	0.0060	0	0.0260	0.0060	0.0010
C. Carmona-C. Morón	0.0100	0.0080	0	0.0380	0.0130	0.0010
C. Carmona-C. Jerez	0.0150	0.0110	0	0.0520	0.0120	0.0010
C. Jerez-C. Morón	0.0060	0.0090	0	0.0180	0.0080	0.0010

Geometrical proportions were used in the past in architectural designs and pictograms related to religious aspects throughout civilizations. Most of them have been built with variables including mathematical numbers, e.g., the golden measure [86]. Moreover, the symbolic geometry includes very identified geometric aspects. For this reason, the geometry proportional to a pattern requires a qualitative and quantitative dimension in the order and shape. Recent studies have assessed textured 3D meshes from the photogrammetry. For instance, [87] established qualitative comparisons of 3D sections, and [88] analyzed the coincidence of 3D curves through the mathematical formulation. For this reason, a second phase of the coincidence analysis of profiles through curves that generated the points in the space of a section plan was carried out (Figure 9).

In this work, profiles are in vertical position, as well as perpendicular to one of the sides of the base of the pillar, in the middle of that side. Afterwards, a referential framework of local coordinates was established before analyzing the profiles. Moreover, this referential framework of local coordinates established the axis "x" as the system in which the characteristic points of the various profiles were aligned, thus maintaining their scale value. Consequently, there were no geometrical limitations, and its coincidence was as adjusted as possible. The spatial distribution of the point group subsets was analyzed in a 2D environment, so the angle θ of the vertical axis was maintained without performing roto-translation. The closest area among curves was calculated to determine both the difference among them and their similarity. Many research works have shown the use of this qualitative methodology. For instance, ref. [89] assessed profiles by extracting the point cloud, so this could be a previous application of the method. Moreover, other studies analyzed both the profile of the areas generated on meshes to calculate the accuracy of campaign series in photograph intakes in the field of photogrammetry [65] and the multidirectional 3D spatial profile to segment individual trees in a hydrographic watershed [90]. It is understood that these are the first studies that analyzed the profiles obtained from the point cloud using the area of the curve with similarity goals in geometrical patterns Figure 10. Although the process could be tedious because points should be extracted and

taken to a statistical software, the analysis is not appropriate to mathematically establish the accuracy of two organic shapes. To verify the solidity of the model within the framework of the mathematical analysis, the points of the curve are used to establish tendency lines in which the mathematical function could be adjusted to the organic shape as maximum as possible. For this purpose, OriginPro 8.5.0 SR1 was used [91].

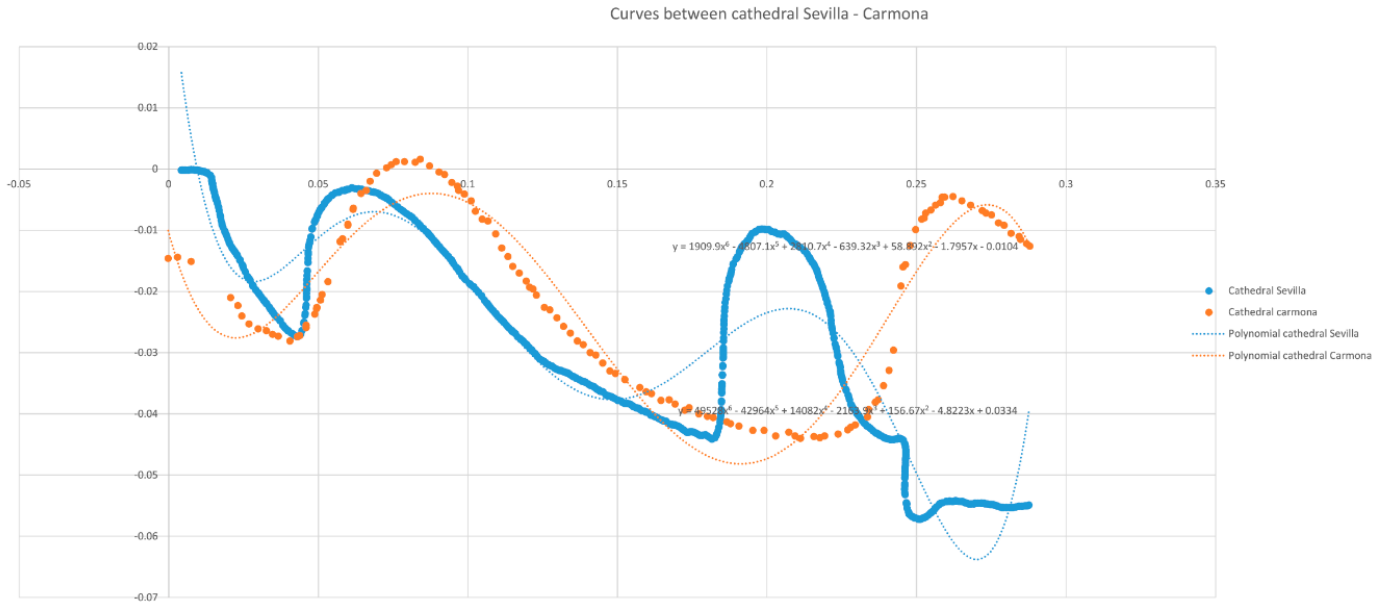

Figure 10. Graph of the curves between the Cathedral of Seville and the church in Carmona.

The subsets of the closest points from profile to profile in the various models created area spaces which were mathematically calculated and the results are show in Table 2. Figure 11 represents the values obtained according to Equation (3).

$$A = \int_a^b f(x)\,dx - \int_a^b g(x)dx \;=\; \int_a^b [f(x) - g(x)]\,dx \tag{3}$$

where A is the differential area between curves, and $f(x)dx$ and $g(x)dx$ are their functions.

Table 2. Table differential area between curves.

Experimental Surveys	Geometric Area (m^2)	Mathematic Area (m^2)	Average Distance	Estimated Standard Error (m)
C. Sevilla-C. Carmona	−0.0014	−0.0013	−0.0014	0.0001
C. Sevilla-C. Morón	−0.0009	−0.0010	−0.0009	0.0001
C. Sevilla-C. Jerez	−0.0013	−0.0015	−0.0014	0.0001
C. Carmona-C. Morón	−0.0022	−0.0017	−0.0019	0.0004
C. Carmona-C. Jerez	−0.0064	−0.0081	−0.0073	0.0012
C. Jerez-C. Morón	−0.0005	−0.0005	−0.0005	0.0000

To know the adjustment of curves, they were structured in parts to know the variability of the areas affected and their relationship between the results of geometrical and mathematical area in each profile.

Assessing the performance of the method proposed is crucial to determine the comparison process between the organic shapes of the Gothic architecture, thus comparing this process with the results of other methods. The lesser the area, the better the estimate.

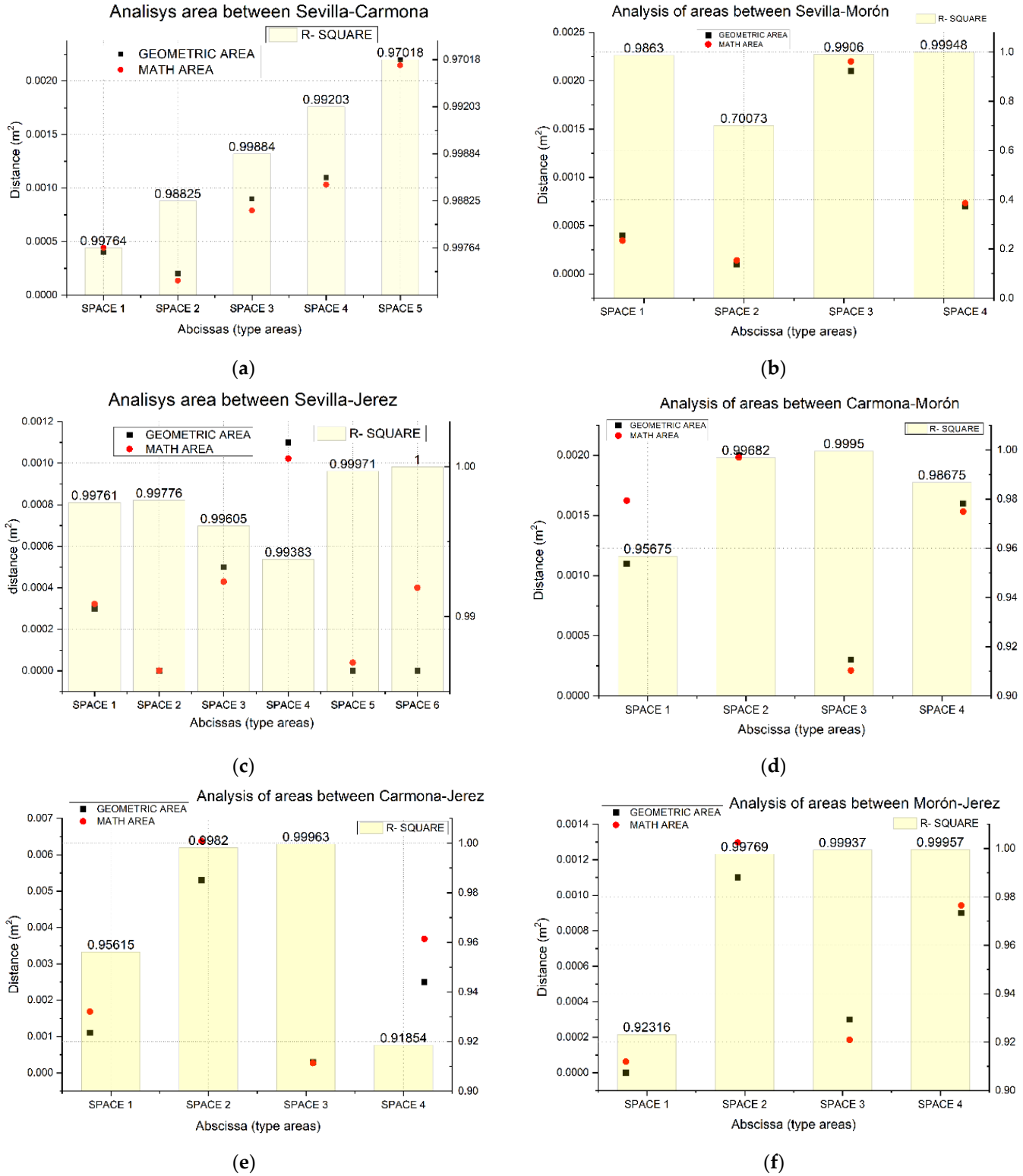

Figure 11. Barplot showing the differential error between the area of the profile and that of each survey: (**a**) Seville and Carmona; (**b**) Seville and Morón; (**c**) Seville and Jerez; (**d**) Carmona and Morón; (**e**) Carmona and Jerez; and (**f**) Morón and Jerez.

The third step is to determine the points that emerge based on repetitive sections in a vertical axis. For this purpose, objects were meshed and divided into vertical and horizontal plans with Rhinoceros [92], following the same criterion and direction in the four case studies (Cathedral of Seville and the churches in Morón, Carmona and Jerez). The

Rhinoceros software allows you to create meshes and generate sections very easily from records obtained by photogrammetry using the e.57 file extension. This software was used since Rhinoceros proves to be the most stable software of the set, among others such as Metashape itself, ClouCompare, and MesLab. According to recent research [65], dections being created for each element were placed on the edges of the horizontal direction and in the middle of the side of each element in vertical direction, as Figure 12 shows.

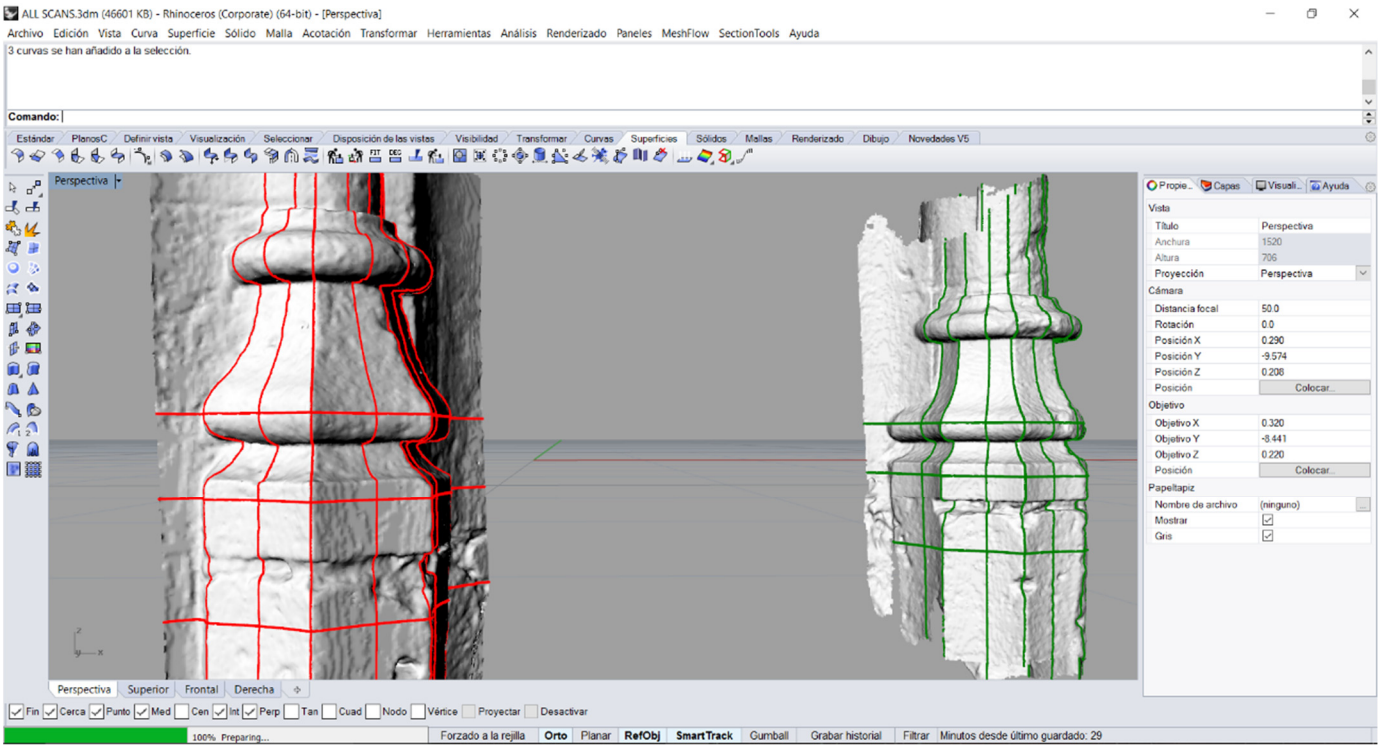

Figure 12. Representation model of horizontal and vertical sections of the bases of the Santiago Church in Jerez de la Frontera.

Results were exported to a 2D coordinate system to adjust the extraction and the characteristic points. In this case, when performing the meshing of the 3D surface, there are no differentials in the form of noise, therefore, making it not difficult to vectorize the architectural sections. Cuts in a 3D model allow the edges to be assessed on sudden changes in the direction of the normal of the triangles of the mesh, thus, according to [93], leading to a reliable interpretation of the model rule.

After comparing through a statistical software, the shapes of the four bases of the cathedral and the churches were analyzed, by using characteristic points, as Figure 13 shows. At this level of detail, the axis of abscissas was doubled to understand the drawing.

The resulting curves were exported to a vector format. Likewise, the coordinates of the characteristic points were extracted for a later mathematical analysis, as Figure 14 shows.

Moreover, the distances between the points of the various profiles were established to better understand the geometric problem, as Figure 15 shows.

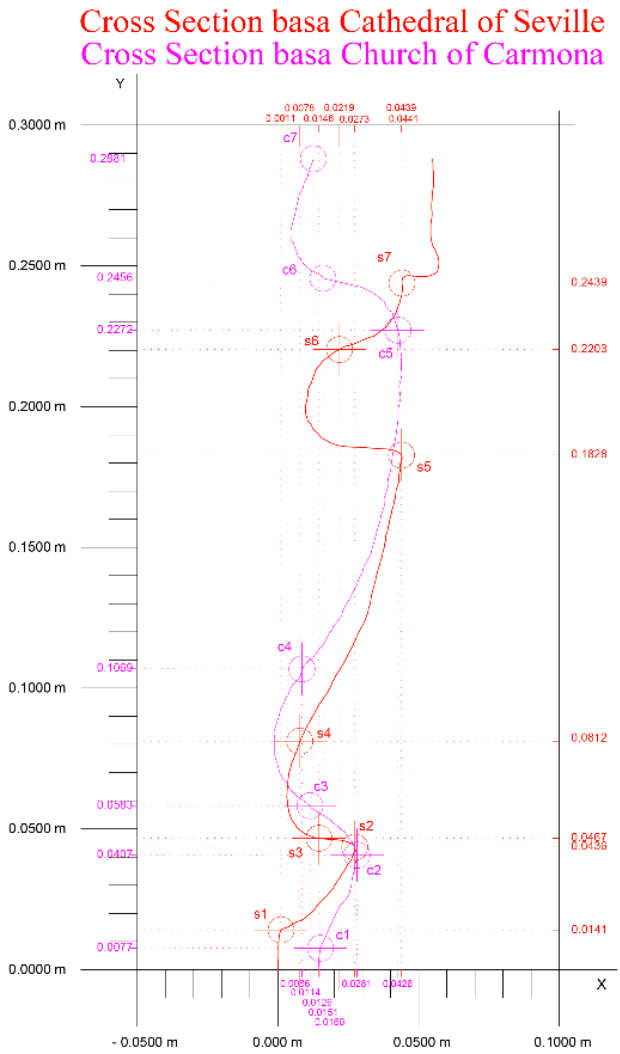

(**a**)

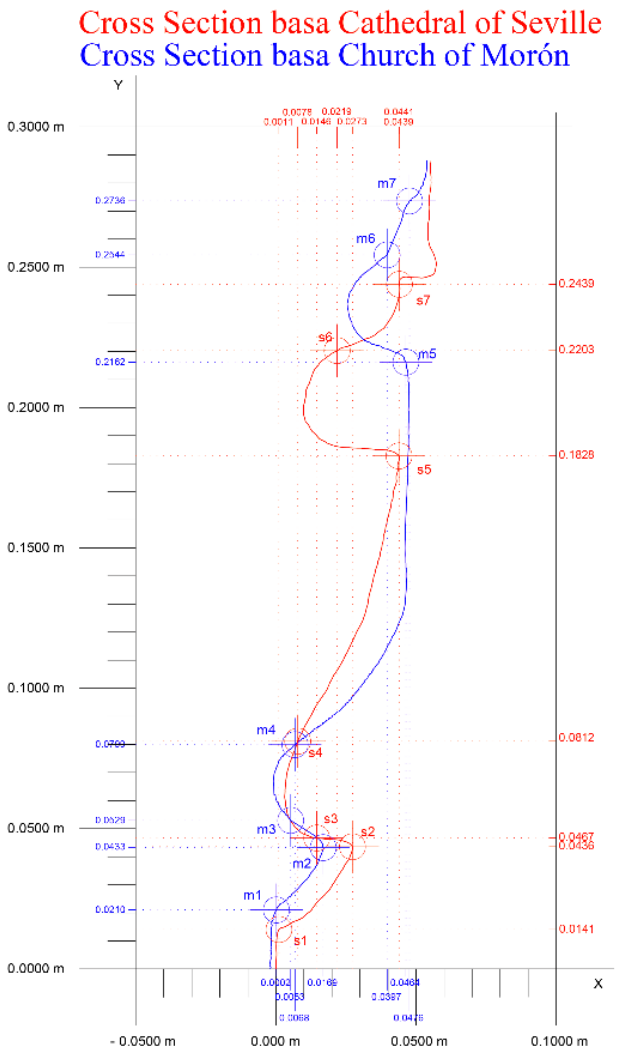

(**b**)

Figure 13. *Cont*.

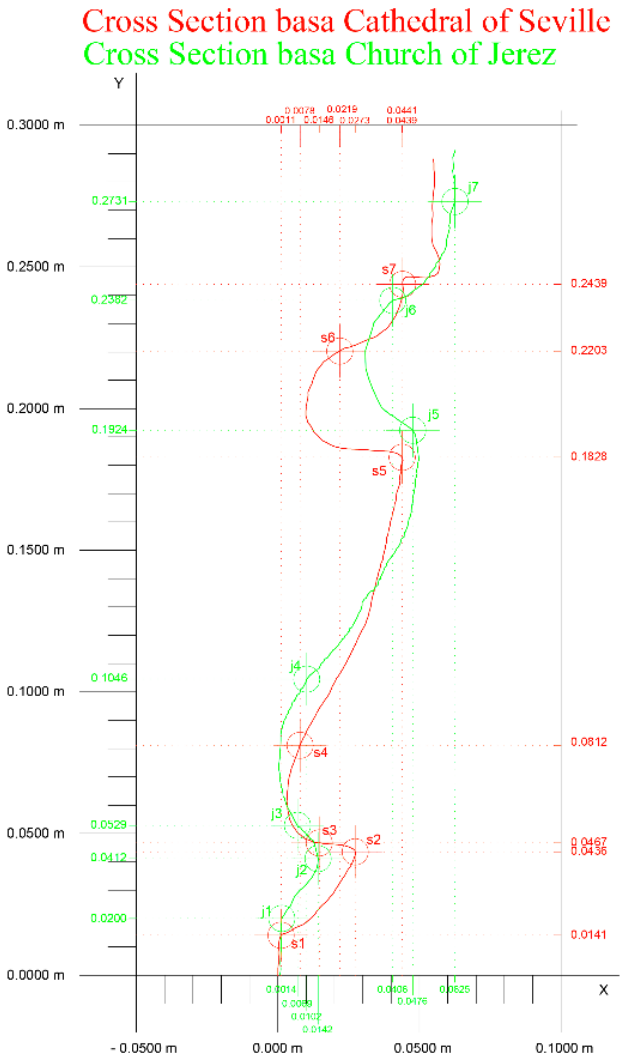

(**c**)

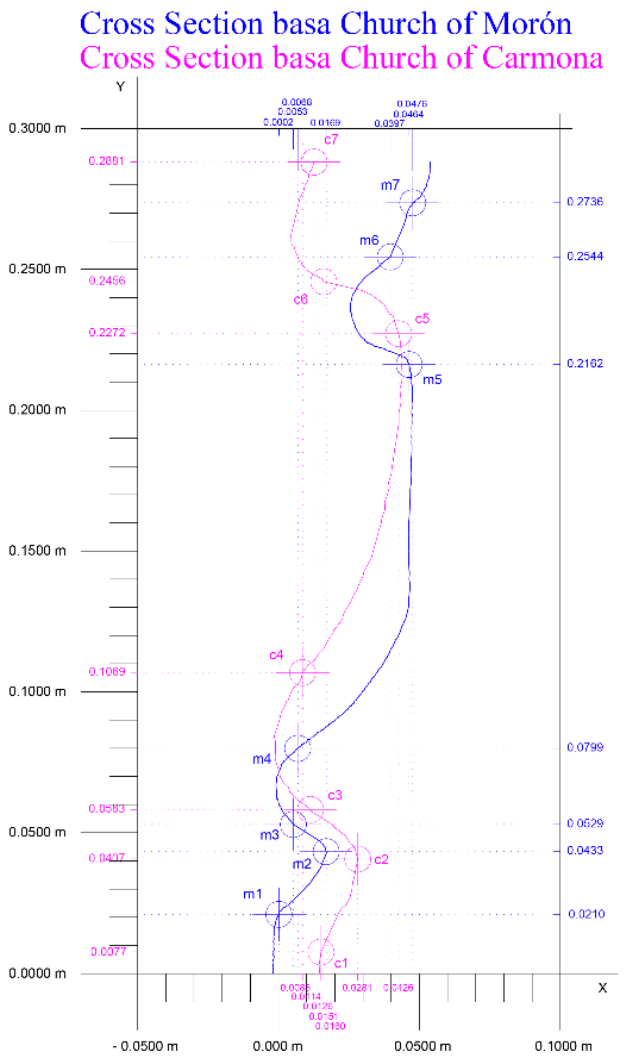

(**d**)

Figure 13. *Cont*.

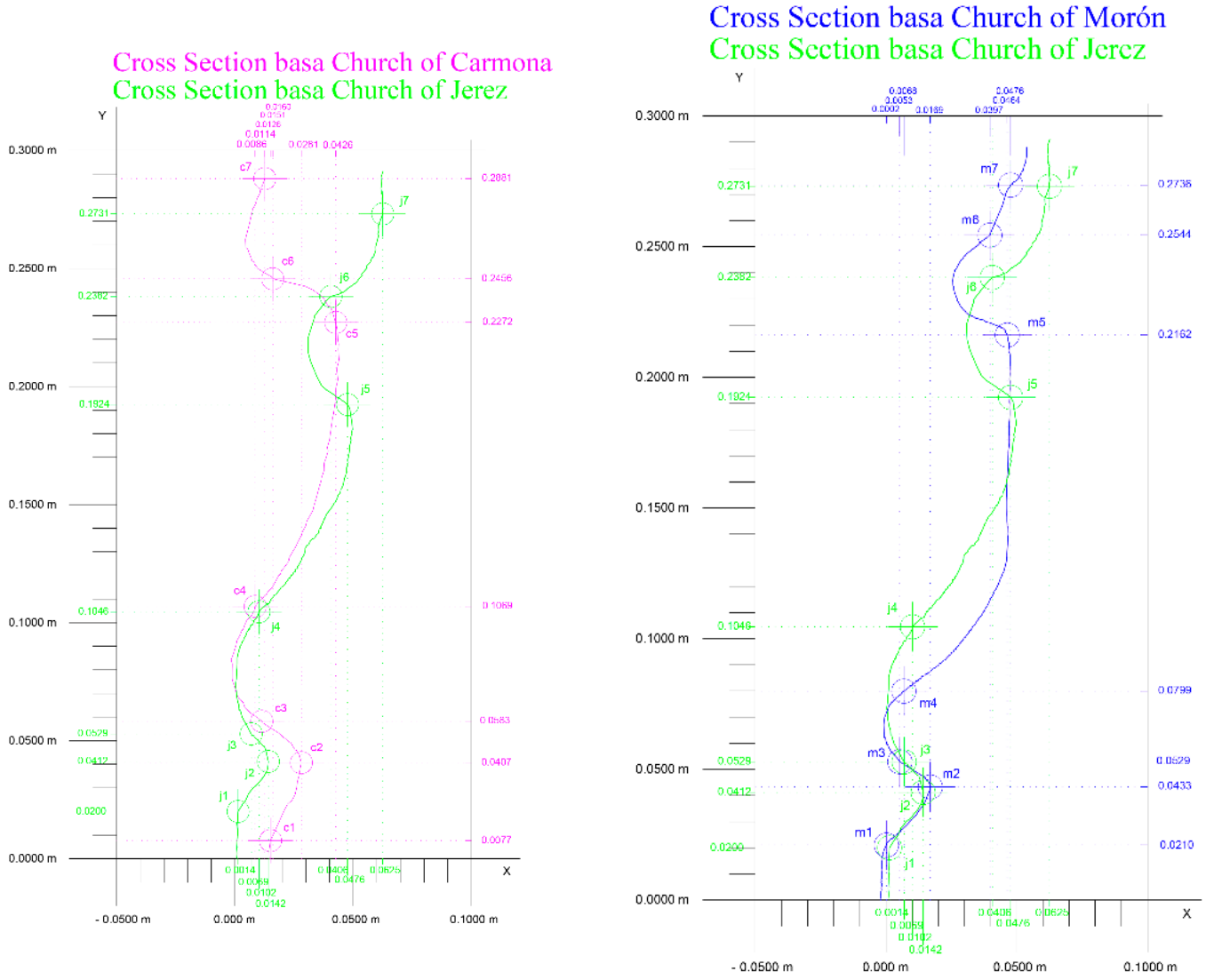

Figure 13. Comparison of sections between the Cathedral of Seville and the churches and their characteristic points: (**a**) Seville and Carmona; (**b**) Seville and Morón; (**c**) Seville and Jerez; (**d**) Carmona and Morón; (**e**) Carmona and Jerez; and (**f**) Morón and Jerez.

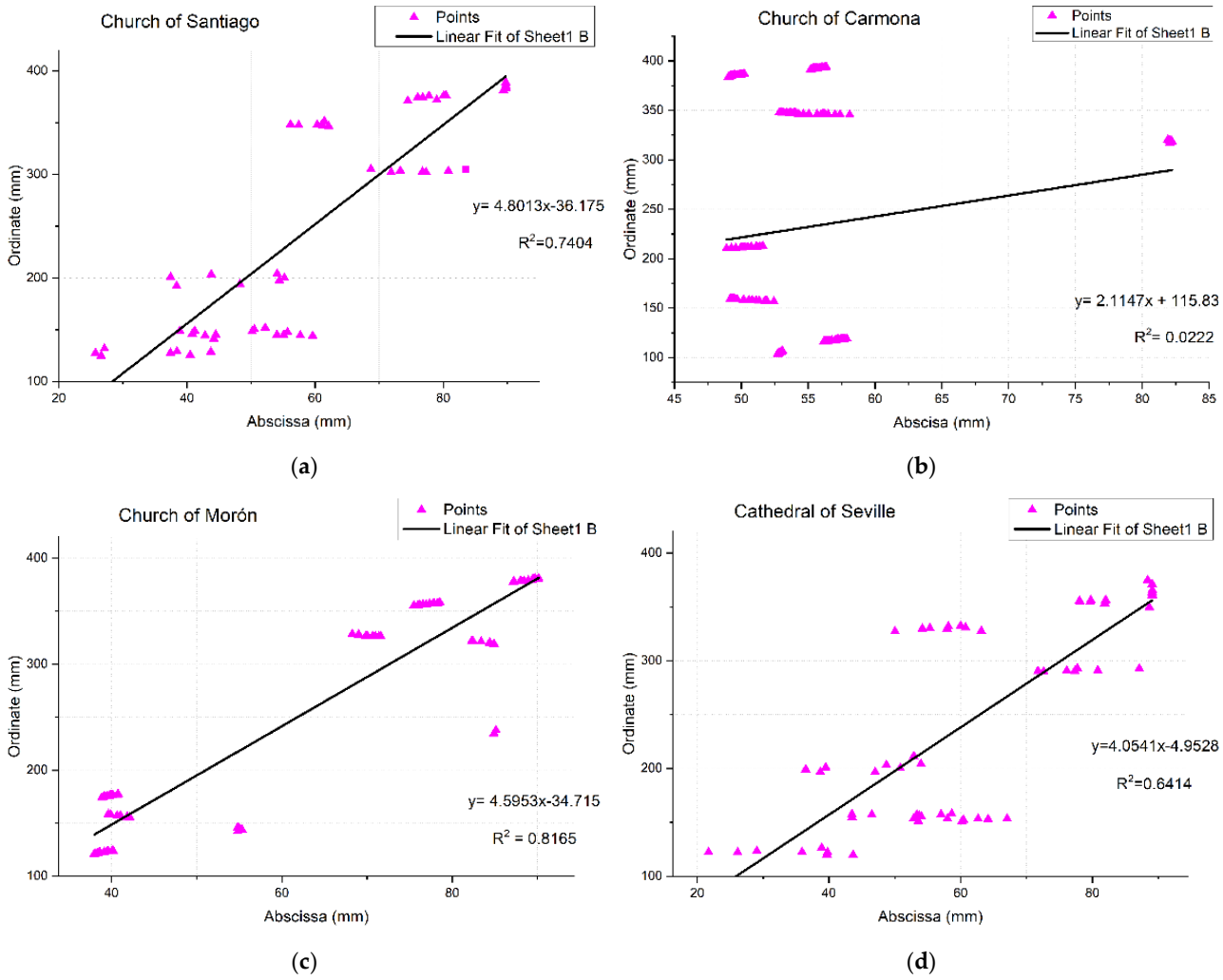

Figure 14. Least squares calculation: (**a**) the Santiago Church, (**b**) the church in Carmona, (**c**) the church in Morón, and (**d**) the Cathedral of Seville.

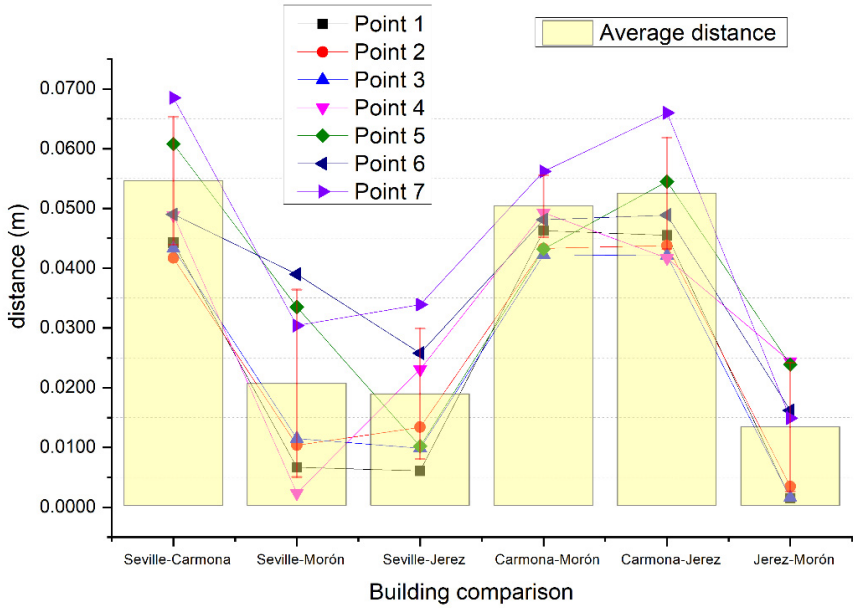

Figure 15. Comparison of the characteristic points.

5. Discussion of Results

Three assessment methods were tested to compare the similarity of the geometrical shapes in the space of Gothic architectural elements. Recent studies have assessed models from the point cloud to compare data acquisition methods, such as TLS and SfM [14,16], multi-camera equipment in a photogrammetric work [94], Simultaneous Localization and Mappings (SLAM) [95], and through algorithms that use C2C as evaluation tools using images captures from Google Earth [96]. Within the various assessment scopes, there is no profile assessment as geometry related to similarity patterns or models. However, characteristic profiles have been identified to explore for the reconstruction of the surface [97] or for goals of 3D modeling [98–100]. Thus, geometric accuracy comparisons were made by calculating the deviation between the point clouds generated by profiles, taking the various patterns as reference. The average deviation among the six types of comparison made an approach of the similarity of the shapes. There were three groups with the lowest estimates in the average distance in meters: firstly, the comparison between the profile of the Cathedral of Seville and the church in Jerez with a value of 0.0063, which is the lowest result; secondly, the Jerez-Morón group with an average distance of 0.0077; and finally, the group between the profiles of Seville-Morón with an average distance of 0.0087 m. Thus, these are the groups in which the greatest distances included in Table 1 obtained the minimum values. The complexity of the method was the extraction of profiles of a same Cartesian system (x, y) because the applicability of the matrix of the translation algorithm of CloudCompare was very complex in a flat surface. To make them coincide and have the greatest correspondence, it was decided to take it to 2D software and finally export it in a .xyz file to CloudCompare.

Although few works have assessed the geometric profiles through the coincidence of curves from reliability and accuracy of the reverse engineering for a geometric pattern, there are more works quantitatively assessing the profiles of textured 3D meshes from photogrammetry [65]. The variation between profiles was established through mathematical analyses with the differentials of the areas according to Equation (3) and through a CAD software to know the geometric area. The results showed first that the geometric and mathematical areas were coincident with a differential of 0.7×10^{-4} m^2, so the mathematical results could be considered valid. On the other hand, the results closer to that value were the comparison between Seville-Morón, with a value of 0.0010 m^2, and Jerez-Morón, with a value of 0.0005 m^2. The standard deviation of the values provided very positive results that showed the adjustment of the mathematical area with the geometric area.

On the other hand, the identification of the characteristic points of a sample determined the similarity correspondence between geometrical shapes. They were used, together with other techniques, for the correspondence of two images in a same scene in the view applications in the computer [101]. The idea was to establish characteristic points based on the opinions of current stonemasons that verify and cut the stone with several tools, such as templates, rules, rigid or articulated squares. These characteristic points determined the patterns of these technical teams to preserve and restore the replica of geometric and organic elements of a Gothic church or cathedral. In the third methodology, and based on the specifications of these characteristic points, the curves of the various bases were exported to a vector format, obtaining the coordinates of the characteristic points to then be analyzed through a linear regression. After adjusting a linear model, the result was four straight lines which showed the percentage of the variation in the variable observed. There is a very similar group, Santiago, Morón, and Seville, with values of R_j^2 of 0.7404, R_M^2 of 0.8165, and R_S^2 of 0.6414, and finally, a more variable result, Carmona, with a R_c^2 of 0.0222. It could be determined in the slope of the straight lines in which that first group had similar slopes. However, the Carmona model had greater dispersion. The reason could be the scalability of the model in contrast to three models with very similar scales and inflections of the curves, and another model was disproportionate as its scale was greater. Moreover, the characteristic points were studied through the differences of the marked

points. The graph showed that the set between Carmona and Jerez was coincident in the low coordinates, as Sevilla-Morón and Sevilla-Jerez.

Figure 14 shows that the models Sevilla-Morón, Sevilla-Jerez, and Jerez-Morón obtained the best pairing results of the characteristic points in the set of average distances. The standard deviation of the analysis was similar, particularly Seville-Jerez had lower values. Figure 16 determines the location of characteristic points and their closeness among them.

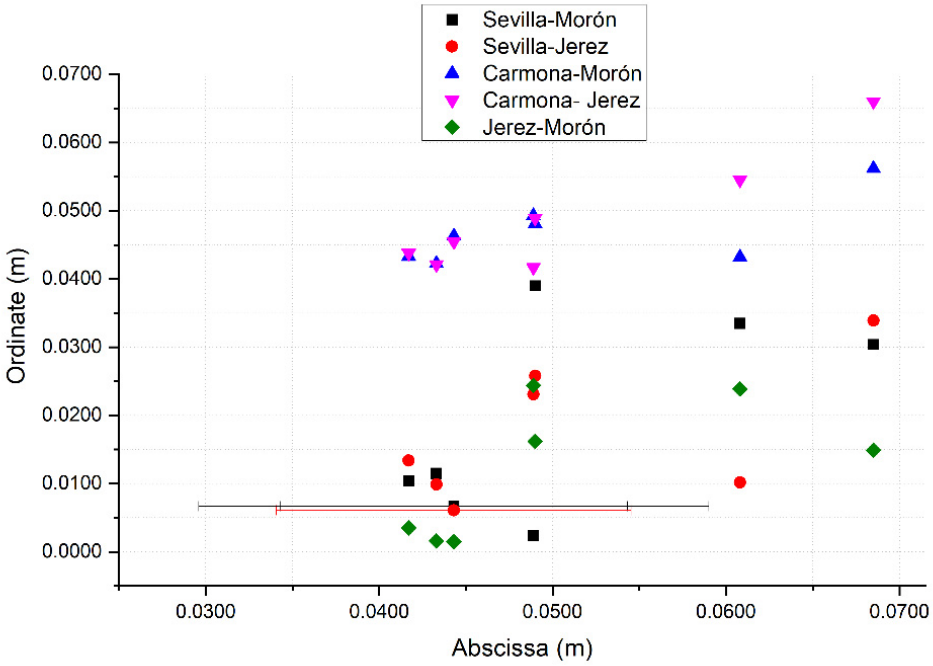

Figure 16. Location of the characteristic points.

The photogrammetry technique provides measurements in the three dimensions of space; length, width, and height of objects in the scene. These measurements are affected by uncertainty [102]. The TLS and SLS datasets were made for presentation purposes, and shape similarity analysis was performed by photogrammetry. However, in this section, we find it interesting to know the deviation associated with these three stated data acquisition techniques. The TLS and SLS dataset and its comparison with the SfM would be useful to know the uncertainty associated with the dataset made in this research. For this work, three sets of SfM_{Xi} points were taken for the photogrammetry registration, SLS_{xi} for the structured light scanner registration, and TLS_{xi} for the terrestrial laser scanner registration. All of them were delimited by two sections of Figure 12 and delimited in their z axis including the drawing of the base. To obtain the uncertainty, three comparisons were made to determine the deviation between the two techniques. According to ISO 3534-1 in metrology, uncertainty is associated with the result of a test that characterizes the range of values within which the true value is found [103]. In this sense, the reference value is found in the values obtained by the results of the SLS_{xi}. The geometric deviation between the records was calculated through the comparison of C2C, once the alignments of the point clouds were made in the same software, obtaining the results of the graph in Figure 17.

The results highlight that photogrammetry is a very solid technique in short-range data capture; therefore, a deviation between photogrammetry values and the structured light scanner of ± 0.00042 m was obtained.

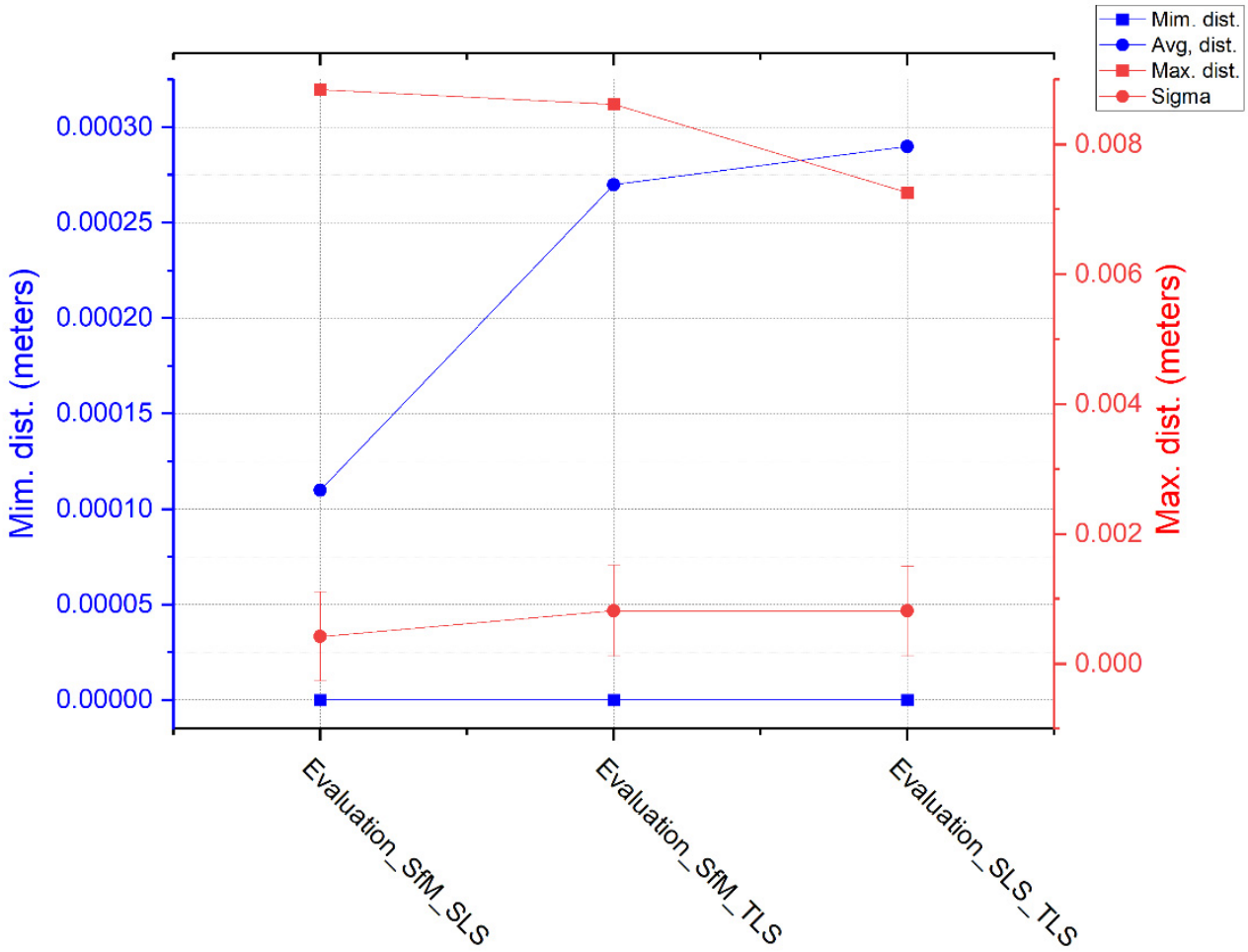

Figure 17. Uncertainty values associated with data acquisition techniques.

6. Conclusions

The progress in digital technologies includes knowledge areas related to both geomatics and techniques of computer vision statistics. These techniques could be useful to represent more and more accurate digital models. In another complementary field, new BIM technologies are considered a new paradigm in architecture, engineering, and cultural heritage. However, there is a new and emergent gap of knowledge in relation to reverse engineering both to analyze architectural shapes and to generate organic geometries to be extracted to BIM models in which metadata related to works conducted in restoration are included.

The scientific literature has shown that massive data acquisition techniques, such as TLS, Optical Scanning (OS), and SfM, have many advantages to show documentary tests on knowledge sources in architectural and archaeological heritage. This study aims at having with photogrammetry techniques to present the many advantages of using SfM to contrast documentary sources in the historical heritage, trying to provide familiarization with the procedures, means, and use of the software for these purposes. In addition, a new approach is proposed to search a geometrical similarity pattern among various architectural elements that are known and that could have a kind of authorship relation.

Satisfactory results were obtained with this technique by generating three-dimensional models, considering that the scientific and academic community accept some errors. Moreover, this data acquisition technology allows an accurate planimetry of reality to be created. All this information was the basis to analyze and to study architectural shapes which have, generally speaking, all the architectural elements of cathedral Gothic buildings, including the pillars studied.

This study is important because it compares some characteristic points of the historical elements to establish their similarity level. The measure variations in scalability, as well as the differentials among the characteristic points between the profile of the church in Carmona and the other buildings suggest the hypothesis that this profile, even similar to the others, differs on authorships of the other Late Gothic churches. The approach of the study was based on three different methodologies, thus providing a new vision to search geometrical similarity patterns to confirm hypotheses initially supported by documentary sources.

Geometries were mathematically interpreted, so it was concluded that the stonemasons of that period used wooden patterns and templates, made by themselves, to cut stones. As for the church in Carmona, it is possible that these templates were not used or that they were deliberately misinterpreted to divide the shapes in their construction. There was a scalability difference of around 80%, so it is possible that this kind of tool was not used.

In addition, the various sections extracted from the SfM technique showed several alterations caused by natural processes, the course of time, human activities, or the structural movements of the buildings during their life cycle. These dimensional inconsistencies were very perceptive, so these bases could be placed, and in situ cut, i.e., not before their placement, as in a normal process. However, some alterations in the elements may have been produced by the own signature of the stonemasons. The speed of construction of the Cathedral of Seville can justify the hypothesis based on the intervention of several stonemasons at the beginning of the works.

The importance of this research lies in establishing a series of characteristic points of historical elements whose authorship is accurately known to compare them with patterns of other objects. These points were established according to the criteria of the current stonemasons.

The characteristic of these architectural elements within the set of cathedrals and churches is crucial because their construction, as the Cathedral of Seville, began by their front and not by their back, unlike other cathedrals. Moreover, the first piece with organic shapes was possibly cut in that period (15th century): the bases of the beginning of the pillar of the cathedral. This would be the first stage of the artistic work developed by the master builder and stonemasons when building a cathedral.

Future research lines could be based on the analysis of other historic buildings to be compared or even the study of other parts of pillars, such as the block of stones in the lower part or their slimness. The pathologies and the erosion of stones over the years could also be studied, thus fulfilling the building life cycle. In fact, this aspect is being studied by the research team led by Professor Fabio Fatiguso at the Polytechnic University of Bari (Italy). In another future line, using image correlation technology, similarity indexes between objects with complex shapes in architecture could be used.

Author Contributions: Conceptualisation, J.M.; Methodology, J.M. and J.E.N.-J.; Software, J.M. and J.E.N.-J.; Validation, J.E.N.-J.; Formal Analysis, J.M. and M.F.-A.; Investigation, J.M. and M.F.-A.; Resources, J.M.; Data Curation, Writing—Original Draft Preparation, J.M. and M.F.-A.; Writing—Review & Editing, J.M., M.F.-A. and J.E.N.-J.; Visualisation, M.J.C.-A. and J.E.N.-J.; Supervision, J.M. and M.J.C.-A.; Project Administration, J.M.; Funding Acquisition, J.M. All authors have read and agreed to the published version of the manuscript.

Funding: This research was funded by Universidad de Sevilla through VI Plan Propio de Investigación y Transferencia (VIPPIT).

Data Availability Statement: Not applicable.

Conflicts of Interest: The authors declare no conflict of interest. The funders had no role in the design of the study; in the collection, analyses, or interpretation of data; in the writing of the manuscript, or in the decision to publish the results.

References

1. Cursi, S.; Simeone, D.; Toldo, I. A semantic web approach for built heritage representation. In Proceedings of the International Conference on Computer-Aided Architectural Design Futures, São Paulo, Brazil, 8–10 July 2015; Volume 527, pp. 383–401.
2. Dore, C.; Murphy, M. Semi-Automatic Modelling of Building Façades with Shape Grammars Using Historic Building Information Modelling. *ISPRS-Int. Arch. Photogramm. Remote Sens. Spat. Inf. Sci.* **2013**, *XL-5/W1*, 57–64. [CrossRef]
3. Pieraccini, M.; Guidi, G.; Atzeni, C. 3D digitizing of cultural heritage. *J. Cult. Herit.* **2001**, *2*, 63–70. [CrossRef]
4. Yilmaz, H.M.; Yakar, M.; Gulec, S.A.; Dulgerler, O.N. Importance of digital close-range photogrammetry in documentation of cultural heritage. *J. Cult. Herit.* **2007**, *8*, 428–433. [CrossRef]
5. Pavlidis, G.; Koutsoudis, A.; Arnaoutoglou, F.; Tsioukas, V.; Chamzas, C. Methods for 3D digitization of Cultural Heritage. *J. Cult. Herit.* **2007**, *8*, 93–98. [CrossRef]
6. Mostaza, T.; Julio, P.J.; Jimeno, Z.; López, J.; Artemio, Q.; Tejera, M. Application of the Scanner Laser 3D to the Spatial Documentation of Archaeological. In Proceedings of the VIII CIA Pósters Teledetección, Teruel, Spain; 2009; pp. 403–408.
7. Mañana-Borrazás, P.; Rodríguez-Paz, A.; Blanco-Rotea, R. An experience in the application of the 3D Laser Scanner to the documentation and analysis processes of Built Heritage: Its application to Santa Eulalia de Bóveda (Lugo) and San Fiz de Solovio (Santiago de Compostela). *Arqueol. Arquit.* **2008**, 15–32. [CrossRef]
8. Almagro Gorbea, A. Planimetry of the Alcazar of Seville. In *Escuela de Estudios Árabes*; CSIC: Granada, Spain, 2000; ISBN 84-7170-166-9.
9. González Muñoz, M.J.; Rueda Ruiz, A.J.; Segura Sánchez, R.J.; Ogáyar Anguita, C.J.; Esteban Hoyas, A.; Lara, J. Use of 3D scanner-based systems for digitization and study of archaeological heritage. *Virtual Archaeol. Rev.* **2010**, *1*, 99. [CrossRef]
10. Capolupo, A. Accuracy Assessment of Cultural Heritage Models Extracting 3D Point Cloud Geometric Features with RPAS SfM-MVS and TLS Techniques. *Drones* **2021**, *5*, 145. [CrossRef]
11. Pepe, M.; Fregonese, L.; Crocetto, N. Use of SfM-MVS approach to nadir and oblique images generated throught aerial cameras to build 2.5D map and 3D models in urban areas. *Geocarto Int.* **2019**, *37*, 120–141. [CrossRef]
12. Tavani, S.; Granado, P.; Riccardi, U.; Seers, T.; Corradetti, A. Terrestrial SfM-MVS photogrammetry from smartphone sensors. *Geomorphology* **2020**, *367*, 107318. [CrossRef]
13. Wenzel, K.; Rothermel, M.; Fritsch, D.; Haala, N.; Wenzel, K.; Rothermel, M.; Fritsch, D.; Haala, N. Image Acquisition and Model Selection for Multi-View Stereo. *ISPAr* **2013**, *XL5*, 251–258. [CrossRef]
14. Teza, G.; Pesci, A.; Ninfo, A. Morphological Analysis for Architectural Applications: Comparison between Laser Scanning and Structure-from-Motion Photogrammetry. *J. Surv. Eng.* **2016**, *142*, 04016004. [CrossRef]
15. Koutsoudis, A.; Vidmar, B.; Ioannakis, G.; Arnaoutoglou, F.; Pavlidis, G.; Chamzas, C. Multi-image 3D reconstruction data evaluation. *J. Cult. Herit.* **2014**, *15*, 73–79. [CrossRef]
16. Westoby, M.J.; Brasington, J.; Glasser, N.F.; Hambrey, M.J.; Reynolds, J.M. 'Structure-from-Motion' photogrammetry: A low-cost, effective tool for geoscience applications. *Geomorphology* **2012**, *179*, 300–314. [CrossRef]
17. Müller, P.; Wonka, P.; Haegler, S.; Ulmer, A.; Van Gool, L. Procedural modeling of buildings. In Proceedings of the ACM SIGGRAPH 2006 Papers, SIGGRAPH '06, Boston, MA, USA, 30 July–3 August 2006; pp. 614–623. [CrossRef]
18. Osello, A. *The future of drawing with BIM for Engineers and Architects*; Dario Flaccovio Editore srl.: Palermo, Italy, 2012; pp. 1–323. Available online: http://www.drawingtothefuture.polito.it/wp-content/uploads/2015/09/abstract_9788857901459-2.pdf (accessed on 28 January 2021).
19. Andreetto, M.; Brusco, N.; Cortelazzo, G.M. Automatic 3-D modeling of textured cultural heritage objects. *IEEE Trans. Image Process.* **2004**, *13*, 354–369. [CrossRef] [PubMed]
20. Girardeau-Montaut, D. CloudCompare Point Cloud Processing Workshop. Available online: www.cloudcompare.org@CloudCompareGPL (accessed on 28 January 2021).
21. Rajendra, Y.D.; Mehrotra, S.C.; Kale, K.V.; Manza, R.R.; Dhumal, R.K.; Nagne, A.D.; Vibhute, A.D.; Rajendra, Y.D.; Mehrotra, S.C.; Kale, K.V.; et al. Evaluation of Partially Overlapping 3D Point Cloud's Registration by using ICP variant and CloudCompare. *ISPAr* **2014**, *40*, 891. [CrossRef]
22. Bassier, M.; Hadjidemetriou, G.; Vergauwen, M. Implementation of Scan-to-BIM and FEM for the Documentation and Analysis of Heritage Timber Roof Structures. *Digit. Herit. Prog. Cult. Herit. Doc. Preserv. Prot.* **2016**, *1*, 79–90. [CrossRef]
23. Moyano, J.; León, J.; Nieto-Julián, J.E.; Bruno, S. Semantic interpretation of architectural and archaeological geometries: Point cloud segmentation for HBIM parameterisation. *Autom. Constr.* **2021**, *130*, 103856. [CrossRef]
24. Zvietcovich, F.; Castaneda, B.; Perucchio, R. 3D solid model updating of complex ancient monumental structures based on local geometrical meshes. *Digit. Appl. Archaeol. Cult. Herit.* **2015**, *2*, 12–27. [CrossRef]
25. Moyano, J.; Gil-Arizón, I.; Nieto-Julián, J.E.; Marín-García, D. Analysis and management of structural deformations through parametric models and HBIM workflow in architectural heritage. *J. Build. Eng.* **2021**, *45*, 103274. [CrossRef]
26. Li, R.; Luo, T.; Zha, H. 3D Digitization and Its Applications in Cultural Heritage. In *Lecture Notes in Computer Science (Including Subseries Lecture Notes in Artificial Intelligence and Lecture Notes in Bioinformatics)*; Springer: Berlin/Heidelberg, Germany, 2010; Volume 6436 LNCS, pp. 381–388. [CrossRef]
27. De Reu, J.; Plets, G.; Verhoeven, G.; De Smedt, P.; Bats, M.; Cherretté, B.; De Maeyer, W.; Deconynck, J.; Herremans, D.; Laloo, P.; et al. Towards a three-dimensional cost-effective registration of the archaeological heritage. *J. Archaeol. Sci.* **2013**, *40*, 1108–1121. [CrossRef]

28. Marín-Buzón, C.; Pérez-Romero, A.M.; León-Bonillo, M.J.; Martínez-álvarez, R.; Mejías-García, J.C.; Manzano-Agugliaro, F. Photogrammetry (SfM) vs. Terrestrial Laser Scanning (TLS) for Archaeological Excavations: Mosaic of Cantillana (Spain) as a Case Study. *Appl. Sci.* **2021**, *11*, 11994. [CrossRef]
29. Tsiafakis, D.; Tsirliganis, N.; Pavlidis, G.; Evangelidis, V.; Chamzas, C. Karabournaki-recording the past: The digitization of an archaeological site. In Proceedings of the International Conference on Electronic Imaging & the Visual Arts EVA 2004, Florence, Italy, 29 March–2 April 2004.
30. Koutsoudis, A.; Chamzas, C. 3D pottery shape matching using depth map images. *J. Cult. Herit.* **2011**, *12*, 128–133. [CrossRef]
31. Zapassky, E.; Finkelstein, I.; Benenson, I. Ancient standards of volume: Negevite Iron Age pottery (Israel) as a case study in 3D modeling. *J. Archaeol. Sci.* **2006**, *33*, 1734–1743. [CrossRef]
32. Karasik, A.; Smilansky, U. 3D scanning technology as a standard archaeological tool for pottery analysis: Practice and theory. *J. Archaeol. Sci.* **2008**, *35*, 1148–1168. [CrossRef]
33. Koutsoudis, A.; Pavlidis, G.; Arnaoutoglou, F.; Tsiafakis, D.; Chamzas, C. Qp: A tool for generating 3D models of ancient Greek pottery. *J. Cult. Herit.* **2009**, *10*, 281–295. [CrossRef]
34. SourceForge QP Real-Time Embedded Frameworks & Tools. Available online: https://sourceforge.net/projects/qpc/files/ (accessed on 28 February 2022).
35. Koutsoudis, A.; Pavlidis, G.; Liami, V.; Tsiafakis, D.; Chamzas, C. 3D Pottery content-based retrieval based on pose normalisation and segmentation. *J. Cult. Herit.* **2010**, *11*, 329–338. [CrossRef]
36. Fiorillo, F.; Remondino, F.; Barba, S.; Santoriello, A.; De Vita, C.B.; Casellato, A. 3D digitization and mapping of heritage monuments and comparison with historical drawings. *ISPRS-Ann. Photogramm. Remote Sens. Spat. Inf. Sci.* **2013**, *II-5/W1*, 2–6. [CrossRef]
37. Hess, M.; MacDonald, L.W.; Valach, J. Application of multi-modal 2D and 3D imaging and analytical techniques to document and examine coins on the example of two Roman silver denarii. *Herit. Sci.* **2018**, *6*, 5. [CrossRef]
38. Bookstein, F.L. Morphometric Tools for Landmark Data Chapter 1. Introduction. In *Morphometric Tools for Landmark Data: Geometry and Biology*; Cambrige University Press: Cambrige, UK, 1991; Volume 435.
39. Zelditch, M.; Swiderski, D.; Sheets, H. *Geometric Morphometrics for Biologists*; Academic Press: Cambridge, MA, USA, 2012. [CrossRef]
40. Shott, M.J.; Trail, B.W. Exploring New Approaches to Lithic Analysis: Laser Scanning and Geometric Morphometrics. *Lithic Technol.* **2016**, *35*, 195–220. [CrossRef]
41. Pintus, R.; Pal, K.; Yang, Y.; Weyrich, T.; Gobbetti, E.; Rushmeier, H. A Survey of Geometric Analysis in Cultural Heritage. *Comput. Graph. Forum.* **2016**, *35*, 4–31. [CrossRef]
42. Xue, F.; Lu, W.; Webster, C.J.; Chen, K. A derivative-free optimization-based approach for detecting architectural symmetries from 3D point clouds. *ISPRS J. Photogramm. Remote Sens.* **2019**, *148*, 32–40. [CrossRef]
43. Herrera Gómez, B.; Samper Sosa, A. Sobre La Fractalidad De Los Rosetones Góticos (About the Fraternity of Gothic Rosettes). In Proceedings of the XII Congreso Internacional Expresión Gráfica aplicada a la Edificación—Graphic Expression applied to Building International Conference—APEGA 2014, Madrid, Spain, 26–28 November 2014; Volume 2, pp. 558–571.
44. Brown, C.T.; Witschey, W.R.T. The fractal geometry of ancient Maya settlement. *J. Archaeol. Sci.* **2003**, *30*, 1619–1632. [CrossRef]
45. Mandelbrot, B.; Mandelbrot, B. *The Fractal Geometry of Nature*; WH Freeman: New York, NY, USA, 1982.
46. Moyano, J.J.; Barrera, J.A.; Nieto, J.E.; Marín, D.; Antón, D. A geometrical similarity pattern as an experimental model for shapes in architectural heritage: A case study of the base of the pillars in the Cathedral of Seville and the church of Santiago in Jerez, Spain. *ISPRS-Int. Arch. Photogramm. Remote Sens. Spat. Inf. Sci.* **2017**, *XLII-2/W3*, 511–517. [CrossRef]
47. López, J.C. *Estereotomía de la Piedra (Stone Stereotomy)*; COAAT: Murcia, Spain, 2004.
48. Cruz Isidoro, F. *Alonso de Vandelvira (1544-ca. 1626/7): Tratadista y Arquitecto Andaluz (Alonso de Vandelvira (1544-ca. 1626/7): Andalusian writer and architect)*; Universidad de Sevilla: Sevilla, Spain, 2001; Volume 316.
49. Morales Martínez, A.J. *Hernán Ruiz "El Joven" (Hernan Ruiz 'The Younger')*; Ediciones Akal: Akal, Madrid, 1996.
50. Capilla Tamborero, E. Hypothesis of geometric methods in profiles of voussoirs of ribbed vaults of the monastery of Santa Maria de la Valldigna (Valencia, Spain). In *Dibujar, Construir, Soñar. Investigaciones en Torno a la Expresión Gráfica Aplicada a la Edificación/Drawing, Building, Dreaming. Research on Graphic Expression Applied to Building*; Tirant lo Blanch: Castellón de la Plana, Spain, 2016; pp. 731–744.
51. Ruiz de la Rosa, J.A. Execution drawings: Documentary value and way of knowledge of the Cathedral of Seville. In *La Catedral Gótica de Sevilla: Fundación y Fábrica de la Obra Nueva*; Universidad de Sevilla: Sevilla, Spain, 2007; pp. 297–348.
52. De Rosa, J.A.R.; Estévez, J.C.R. *Round Chapel in a Round Round: New Contributions on a Renaissance Hill in the Cathedral of Seville*; Universidad de Sevilla: Sevilla, Spain, 2011.
53. López Mozo, A.; Rabasa Díaz, E.; Sobrino González, M. The line in the material control of the form. In Proceedings of the Actas del Séptimo Congreso Nacional de Historia de la Construcción, Santiago de Compostela, Santiago, CA, USA, 26–29 October 2011; pp. 743–754.
54. Boschert, S.; Rosen, R.; Boschert, S.; Rosen, R. Digital Twin—The Simulation Aspect. In *Mechatronic Futures: Challenges and Solutions for Mechatronic Systems and Their Designers*; Springer International: Heidelberg, Germany, 2016; pp. 59–74. [CrossRef]

55. Caramazana Malia, D.; Romero Bejarano, M. New data on "the Gothic facades of Cadiz": The patronage of Cardinal Diego Hurtado de Mendoza in the parish of Santiago de Jerez and the authorship of Rodrigo de Alcalá in the parish of San Jorge de Alcalá de los Gazules. *Lab. Arte* **2016**, *28*, 41–60. [CrossRef]
56. Falcón Márquez, T. *The Gothic Building, the Cathedral of Seville*; Guadalquivir, S.L., Ed.; Ediciones: Sevilla, Spain, 1991.
57. Pinto Puerto, F.; Guerrero Vega, J.M. Estudios previos a la intervención en la capilla de la antigua iglesia de San Miguel, en Morón de la Frontera (Sevilla) (Studies prior to the intervention in the chapel of the old church of San Miguel, in Morón de la Frontera (Seville)). *Arqueol. Arquit.* **2009**, *6*, 267–286. [CrossRef]
58. Ojeda Barrera, A. The work of the primitive chapel of the Tabernacle of Santa María de Carmona. *Lab. Arte* **2014**, *26*, 73–93.
59. Pomar Rodil, P.J. La pervivencia de la técnica medieval en la arquitectura andaluza: La Catedral de Jerez de la Frontera (Cádiz), una construcción "gótica" del pleno Barroco. In Proceedings of the Actas del Tercer Congreso Nacional de Historia de la Construcción, Sevilla, Spain, 26–28 October 2000; Volume 2, pp. 841–852, ISBN 84-95365-56-1.
60. Juan Carlos RUIZ SOUZA y Antonio GARCÍA FLORES Ysambart y la renovación del gótico final en Castilla: Palencia, la Capilla del Contador Saldaña en Tordesillas y Sevilla. Hipótesis para el debate. *An. De Hist. Del Arte* **2009**, *19*, 43–76.
61. Coveney, S.; Stewart Fotheringham, A.; Charlton, M.; McCarthy, T. Dual-scale validation of a medium-resolution coastal DEM with terrestrial LiDAR DSM and GPS. *Comput. Geosci.* **2010**, *36*, 489–499. [CrossRef]
62. Forlani, G.; Pinto, L.; Roncella, R.; Pagliari, D. Terrestrial photogrammetry without ground control points. *Earth Sci. Inform.* **2014**, *7*, 71–81. [CrossRef]
63. dos Santos, D.R.; Dal Poz, A.P.; Khoshelham, K. Indirect Georeferencing of Terrestrial Laser Scanning Data using Control Lines. *Photogramm. Rec.* **2013**, *28*, 276–292. [CrossRef]
64. Akca, D.; Freeman, M. Quality assessment of 3D building data. *Photogramm. Rec.* **2010**, *25*, 339–355. [CrossRef]
65. Moyano, J.; Nieto-Julián, J.E.; Bienvenido-Huertas, D.; Marín-García, D. Validation of Close-Range Photogrammetry for Architectural and Archaeological Heritage: Analysis of Point Density and 3d Mesh Geometry. *Remote Sens.* **2020**, *12*, 3571. [CrossRef]
66. Gonçalves, J.A.; Henriques, R. UAV photogrammetry for topographic monitoring of coastal areas. *ISPRS J. Photogramm. Remote Sens.* **2015**, *104*, 101–111. [CrossRef]
67. Campos, M.; Tommaselli, A.; Ivánová, I.; Billen, R. Data Product Specification Proposal for Architectural Heritage Documentation with Photogrammetric Techniques: A Case Study in Brazil. *Remote Sens.* **2015**, *7*, 13337–13363. [CrossRef]
68. David, P.H. Darktable. Available online: https://www.darktable.org/ (accessed on 30 January 2020).
69. Agisoft PhotoScan Software. Agisoft Metashape. Available online: https://www.agisoft.com/ (accessed on 30 January 2020).
70. Geosystems Leica Geosystems (2008) Leica FlexLine TS02/TS06/TS09 User Manual. Available online: https://leica-geosystems.com/ (accessed on 16 March 2020).
71. Moyano, J.; Nieto-Julián, J.E.; Antón, D.; Cabrera, E.; Bienvenido-Huertas, D.; Sánchez, N. Suitability Study of Structure-from-Motion for the Digitisation of Architectural (Heritage) Spaces to Apply Divergent Photograph Collection. *Symmetry* **2020**, *12*, 1981. [CrossRef]
72. Jaud, M.; Passot, S.; Allemand, P.; Le Dantec, N.; Grandjean, P.; Delacourt, C. Suggestions to Limit Geometric Distortions in the Reconstruction of Linear Coastal Landforms by SfM Photogrammetry with PhotoScan® and MicMac® for UAV Surveys with Restricted GCPs Pattern. *Drones* **2019**, *3*, 2. [CrossRef]
73. Guarnieri, A.; Remondino, F.; Vettore, A. Digital Photogrammetry and Tls Data Fusion Applied To Cultural Heritage 3D Modeling. *Int. Arch. Photogramm. Remote Sens. Spat. Inf. Sci.* **2006**, *36*, 1–6.
74. Seminati, E.; Talamas, D.C.; Young, M.; Twiste, M.; Dhokia, V.; Bilzon, J.L.J. Validity and reliability of a novel 3D scanner for assessment of the shape and volume of amputees' residual limb models. *PLoS ONE* **2017**, *12*, e0184498. [CrossRef]
75. Psikuta, A.; Frackiewicz-Kaczmarek, J.; Mert, E.; Bueno, M.A.; Rossi, R.M. Validation of a novel 3D scanning method for determination of the air gap in clothing. *Measurement* **2015**, *67*, 61–70. [CrossRef]
76. Kim, D.H.; Gratchev, I. Application of Optical Flow Technique and Photogrammetry for Rockfall Dynamics: A Case Study on a Field Test. *Remote Sens.* **2021**, *13*, 4124. [CrossRef]
77. Hild, F.; Roux, S. Comparison of Local and Global Approaches to Digital Image Correlation. *Exp. Mech.* **2012**, *52*, 1503–1519. [CrossRef]
78. Chou, P.A.; Koroteev, M.; Krivokuca, M. A Volumetric Approach to Point Cloud Compression—Part I: Attribute Compression. *IEEE Trans. Image Process.* **2020**, *29*, 2203–2216. [CrossRef]
79. Mémoli, F.; Sapiro, G. Comparing Point Clouds. In Proceedings of the 2004 Eurographics/ACM SIGGRAPH Symposium on Geometry Processing—SGP, Nice, France, 8–10 July 2004. [CrossRef]
80. Agisoft PhotoScan Software. Agisoft PhotoScan. Available online: https://www.agisoft.es/products/agisoft-photoscan/ (accessed on 9 May 2019).
81. Antón, D.; Medjdoub, B.; Shrahily, R.; Moyano, J. Accuracy evaluation of the semi-automatic 3D modeling for historical building information models. *Int. J. Archit. Herit.* **2018**, *12*, 790–805. [CrossRef]
82. Arias, P.; Ordóñez, C.; Lorenzo, H.; Herraez, J. Methods for documenting historical agro-industrial buildings: A comparative study and a simple photogrammetric method. *J. Cult. Herit.* **2006**, *7*, 350–354. [CrossRef]
83. Lane, S.N.; James, T.D.; Crowell, M.D. Application of digital photogrammetry to complex topography for geomorphological research. *Photogramm. Rec.* **2000**, *16*, 793–821. [CrossRef]
84. Pielke, R.A. *Mesoscale Meteorological Modeling*, 3rd ed.; Academic Press: Cambridge, UK, 1984.

85. Olivier, M.D.; Robert, S.; Richard, A.F. A method to quantify canopy changes using multi-temporal terrestrial lidar data: Tree response to surrounding gaps. *Agric. For. Meteorol.* **2017**, *237*, 184–195. [CrossRef]
86. Dabbour, L.M. Geometric proportions: The underlying structure of design process for Islamic geometric patterns. *Front. Archit. Res.* **2012**, *1*, 380–391. [CrossRef]
87. Chiabrando, F.; Lingua, A.; Noardo, F.; Spanò, A. 3D modelling of trompe l'oeil decorated vaults using dense matching techniques. *Int. Arch. Photogramm Remote Sens. Spat. Inf. Sci.* **2014**, *2*, 97–104. [CrossRef]
88. Gruen, A.; Akca, D. Least squares 3D surface and curve matching. *ISPRS J. Photogramm. Remote Sens.* **2005**, *59*, 151–174. [CrossRef]
89. Remondino, F.; Spera, M.; Nocerino, E. State of the art in high density image matching. *Photogramm. Rec.* **2014**, *29*, 144–166. [CrossRef]
90. Yang, J.; Kang, Z.; Cheng, S.; Yang, Z.; Akwensi, P.H. An Individual Tree Segmentation Method Based on Watershed Algorithm and Three-Dimensional Spatial Distribution Analysis From Airborne LiDAR Point Clouds. *IEEE J. Sel. Top. Appl. Earth Obs. Remote Sens.* **2020**, *13*, 1055–1067. [CrossRef]
91. *OriginLab OriginPro—Data Analysis and Graphing Software*; OriginLab: Northampton, MA, USA, 2021.
92. Robert McNeel & Associates Rhinoceros. Available online: https://www.rhino3d.com/ (accessed on 27 March 2020).
93. Gines, J.L.C.; Cervera, C.B. Toward Hybrid Modeling and Automatic Planimetry for Graphic Documentation of the Archaeological Heritage: The Cortina Family Pantheon in the Cemetery of Valencia. *Int. J. Archit. Herit.* **2019**, *14*, 1210–1220. [CrossRef]
94. Teppati Losè, L.; Chiabrando, F.; Spanò, A.; Teppati Losè, L.; Chiabrando, F.; Spanò, A. Preliminary Evaluation of a Commercial 360 Multi-Camera Rig for Photogrammetric Purposes. *ISPAr* **2018**, *422*, 1113–1120. [CrossRef]
95. Wang, J.; Shahbazi, M.; Wang, J.; Shahbazi, M. Mapping Quality Evaluation of Monocular Slam Solutions for Micro Aerial Vehicles. *ISPAr* **2019**, *4217*, 413–420. [CrossRef]
96. Marques, A.; Kenji Horota, R.; De Souza, E.M.; Rossa, P.; Aires, A.S.; Roberto Veronez, M.; Gonzaga, L.; Lessio Cazarin, C. Skewness-Adjusted Robust Statistical Assessment on Googles Earth 3D Models: Rapplee Ridge. In Proceedings of the International Geoscience and Remote Sensing Symposium (IGARSS), Yokohama, Japan, 28 July–2 August 2019; pp. 4348–4351. [CrossRef]
97. De Luca, L.; Veron, P.; Florenzano, M. Reverse engineering of architectural buildings based on a hybrid modeling approach. *Comput. Graph.* **2006**, *30*, 160–176. [CrossRef]
98. Brumana, R.; Oreni, D.; Raimondi, A.; Georgopoulos, A.; Bregianni, A. From survey to HBIM for documentation, dissemination and management of built heritage: The case study of St. Maria in Scaria d'Intelvi. In Proceedings of the 2013 Digital Heritage International Congress (DigitalHeritage), Marseille, France, 28 October–1 November 2013; Volume 1, pp. 497–504.
99. David Lo Buglio, L.D.L. Representation of architectural artifacts definition of an approach combining the complexity of the 3D digital instance with the intelligibility of the theoretical model. *Sci. Res. Inf. Technol.* **2012**, *2*, 63–76. [CrossRef]
100. Tommasi, C.; Achille, C.; Fassi, F. From point cloud to BIM: A modelling challenge in the Cultural Heritage field. *Isprs-Int. Arch. Photogramm. Remote Sens. Spat. Inf. Sci.* **2016**, *XLI-B5*, 429–436. [CrossRef]
101. Bay, H.; Ess, A.; Tuytelaars, T.; Van Gool, L. Speeded-Up Robust Features (SURF). *Comput. Vis. Image Underst.* **2008**, *110*, 346–359. [CrossRef]
102. Daponte, P.; De Vito, L.; Mazzilli, G.; Picariello, F.; Rapuano, S. A height measurement uncertainty model for archaeological surveys by aerial photogrammetry. *Measurement* **2017**, *98*, 192–198. [CrossRef]
103. Ramón Parra-Michel, J.; Martínez García, A.; Martínez, J.A. Standard uncertainty calculation by Monte Carlo technique for topography and hole-filed displacement measurement means ESPI. *Nova Sci.* **2013**, *5*, 51–75.